



Geometric stability switch criteria in delay differential equations with two delays and delay dependent parameters [☆]

Qi An ^a, Edoardo Beretta ^b, Yang Kuang ^c, Chuncheng Wang ^a,
Hao Wang ^{d,*}

^a Department of Mathematics, Harbin Institute of Technology, Harbin, Heilongjiang, 150001, China

^b CIMAB: Interuniversity Centre for Mathematics Applied to Biology, Medicine and Environmental Sciences, Italy

^c School of Mathematical and Statistical Sciences, Arizona State University, Tempe, AZ, 85287-1804, USA

^d Department of Mathematical and Statistical Sciences, University of Alberta, Edmonton, Alberta, T6G 2G1, Canada

Received 20 September 2018; revised 9 November 2018

Abstract

Most modeling efforts involve multiple physical or biological processes. All physical or biological processes take time to complete. Therefore, multiple time delays occur naturally and shall be considered in more advanced modeling efforts. Carefully formulated models of such natural processes often involve multiple delays and delay dependent parameters. However, a general and practical theory for the stability analysis of models with more than one discrete delay and delay dependent parameters is nonexistent. The main purpose of this paper is to present a practical geometric method to study the stability switching properties of a general transcendental equation which may result from a stability analysis of a model with two discrete time delays and delay dependent parameters that dependent only on one of the time delay. In addition to simple and illustrative examples, we present a detailed application of our method to the study of a two discrete delay SIR model.

© 2018 Elsevier Inc. All rights reserved.

[☆] This work is partially supported by a Chinese NSF grant 11671110, a US NSF grant DMS-1615879, and a Canadian NSERC grant RGPIN-2015-04581.

* Corresponding author.

E-mail addresses: anqi@stu.hit.edu.cn (Q. An), e.beretta@mat.uniurb.it (E. Beretta), kuang@asu.edu (Y. Kuang), wangchuncheng@hit.edu.cn (C. Wang), hao8@ualberta.ca (H. Wang).

<https://doi.org/10.1016/j.jde.2018.11.025>

0022-0396/© 2018 Elsevier Inc. All rights reserved.

MSC: 34K18; 34K20; 92D30

Keywords: Delay differential equation; Stability switch; Characteristic equation; Epidemic model

1. Introduction

All physical and biological processes take time to complete. In almost all the modeling efforts that involving multiple physical and/or biological processes, multiple time delays occur naturally [1–4]. There are three popular ways of incorporating time delays in a mathematical model involving physical or biological processes. Time delays can and are often introduced through multiple compartments in compartmental models [5,6]. Time delays can appear naturally via aggregations in structured mathematical models such as age, stage or size structured population models [7–10]. Of course, time delays can also be incorporated in models directly in mostly ad hoc ways [11,12].

Direct ways of incorporating time delays in biological models, while intuitive and practical, can be problematic both mathematically and biologically. For an example, the well known Hutchinson model (also known as the delayed logistic equation with a discrete delay),

$$\frac{dx(t)}{dt} = rx(t) \left(1 - \frac{x(t-\tau)}{K} \right),$$

where the parameters r , K and τ are often referred to as a population growth rate (birth rate b minus death rate d), environment carrying capacity and population growth delay. If we take a closer look at the time delay, we will find it is almost impossible to convincingly associate it with any well defined biological concept. To see this, we can rewrite the Hutchinson model as

$$\frac{dx(t)}{dt} = rx(t) - r \frac{x(t)x(t-\tau)}{K}. \quad (1.1)$$

The first term represents the growth rate of population when density is low and negligible. The second term represents reduction of growth due to crowding effect when time delay is absent. However, with the presence of time delay, it has no clear biological meaning since the present population $x(t)$ can not interact with past population $x(t-\tau)$. Even if we can make additional assumption to make sense out of it, we must assume the interactions is between the current population $x(t)$ and the surviving population existed τ units time ago (which is $e^{-d\tau}x(t-\tau)$, where $e^{-d\tau}$ is the survive rate of individual existed τ units of time ago). In addition, it is well known that the amplitude of oscillatory solutions of (1.1) increases rapidly as $r\tau$ passes through $\pi/2$, leading to solutions with extremely large maximum value, and a minimum close to zero (see Figure 1 in [13]).

In most situations where time delay plays an important role in shaping the observed complex dynamics, small time delays usually are harmless to a stable system while larger time delays may destabilize it [14–18]. This is also clear for the Hutchinson model where small positive solutions tend to the carrying capacity when $r\tau < \pi/2$ [2]. However, for delay differential equation models resulting from age structure models or careful formulations, time delays often appear in the survive rates (such as $e^{-d\tau}$) of the delayed populations [19]. These models are called models with delay dependent parameters (or delay-dependent coefficients). For such models, it is now well known that time delay in can be both stabilizing and destabilizing, depending on the delay

lengths [19]. The work of Beretta and Kuang [19] was extended and enriched in various ways and found many applications beyond life sciences [20]. More recent applications in the context of partial differential equation models with delay dependent parameters and global bifurcation analysis can be found in [21,22]. For a timely and comprehensive review of the theory and applications of models with only one discrete delay and delay dependent parameters, see [23]. We would like to mention that when delays do not appear in parameters, there are a few well known results on the stability of delay differential equations with two delays [24–28]. In 2003, Beretta and Tang extended the work of Beretta and Kuang (2002) to study systems of delay differential equations with a single time delay [29]. However, given the ubiquitous presence of multiple time delays in a complex biological process, a general and practical theory for models with more than one discrete delay and delay dependent parameters is urgently needed.

The main purpose of this paper is to extend the geometric method introduced in [5] to study the stability switching properties of a general transcendental equation which may result from a stability analysis of a model with two discrete time delays and delay dependent parameters that dependent only on one of the time delay. We present our key assumptions in the next section, followed by a detailed section on the rich behavior of crossing curve. In section 4, we present practical conditions that determine crossing directions for imaginary roots of the general transcendental equation with two time delay and delay dependent coefficients. With the help of our general result, a detailed analysis of a two discrete delay SIR model is presented in section 5. We end this paper with a brief section summarizing the key steps in determining the crossing curves and show some other applications of this geometric method. Several examples for demonstrating different types of crossing curve are provided in Appendix A.

2. Assumptions

In this section, we present a general transcendental equation, given by (2.1), that frequently arises from two-delay differential equations with one-delay dependent coefficients. We provide the basic assumptions for studying the crossing curves of (2.1).

Let \mathbb{R}_+ , \mathbb{N}_0 , \mathbb{Z} and \mathbb{C} be the sets of nonnegative real numbers, nonnegative integer numbers, integer numbers and complex numbers, respectively. For any $z \in \mathbb{C}$, denote by $\arg(z)$ the principal value of the argument of z in the interval $(-\pi, \pi]$.

Consider the following transcendental equation

$$D(\lambda, \tau, \tau_1) := P_0(\lambda, \tau) + P_1(\lambda, \tau)e^{-\lambda\tau} + P_2(\lambda, \tau)e^{-\lambda\tau_1} = 0, \quad (2.1)$$

where $\tau \in I \subseteq \mathbb{R}_+$, $\tau_1 \in \mathbb{R}_+$, $P_l(\lambda, \tau)$, $l = 0, 1, 2$ are polynomials in λ whose coefficients, say $p_{kl}(\tau)$, are bounded functions $p_{kl} : I \rightarrow \mathbb{R}$ of class C^1 . For a differential equation with two time delays and parameters depending on one of the delays, the characteristic equation at an equilibrium E may often take the form of (2.1). In this paper, we will focus on the distribution of roots for (2.1), and study how the roots vary as the two time delays τ, τ_1 are changed. In particular, we are about to determine the curves, referred as “crossing curves”, on (τ, τ_1) -plane, on which (2.1) has purely imaginary roots.

When $P_l(\lambda, \tau)$, $l = 0, 1, 2$ are independent of the delay τ , the crossing curves can be obtained by a geometric method, established in [5]. It is our intention to extend this method to (2.1), finding out what kind of crossing curves that (2.1) may have. We make the following basic assumptions:

(H1) Existence of a principal term: $\deg(P_0(\lambda, \tau)) \geq \max\{\deg(P_1(\lambda, \tau)), \deg(P_2(\lambda, \tau))\}$;

- (H2) No zero frequency: $P_0(0, \tau) + P_1(0, \tau) + P_2(0, \tau) \neq 0$ for any $\tau \in I$;
 (H3) The polynomials $P_l(\lambda, \tau)$, $l = 0, 1, 2$ have no common factor;
 (H4) No large oscillation: $\lim_{|\lambda| \rightarrow \infty} \sup_{\substack{\text{Re} \lambda \geq 0 \\ \tau \in I}} \left(\left| \frac{P_1(\lambda, \tau)}{P_0(\lambda, \tau)} \right| + \left| \frac{P_2(\lambda, \tau)}{P_0(\lambda, \tau)} \right| \right) < 1$;
 (H5) $P_l(i\omega; \tau) \neq 0$, $l = 0, 1, 2$, for any $\tau \in I$ and $\omega \in \mathbb{R}_+$;
 (H6) For any $\omega \in \mathbb{R}_+$, at least one of $|P_l(i\omega, \tau)|$, $l = 0, 1, 2$ tends to ∞ as $\tau \rightarrow -\infty$. If there are multiple such P_l , then these functions tend to infinity at different rates.

The items (H1)–(H3) are analogous to assumptions (I)–(III) in [5]. If (H1) is not satisfied, there are always roots in the right hand side complex plane. (H2) will rule out the possibility that 0 is a zero of (2.1) for any $(\tau, \tau_1) \in I \times \mathbb{R}_+$. If (H3) is violated, then (2.1) can be written as the product of another transcendental equation satisfying (H3) and $c(\lambda, \tau)$, where $c(\lambda, \tau)$ is a common factor of $P_l(\lambda, \tau)$, $l = 0, 1, 2$. (H4) is slightly different from (IV) in [5], in that $P_l(\lambda, \tau)$, $l = 0, 1, 2$ are now delay-dependent. It will be seen below that (H4) precludes $i\omega$ is a root of (2.1) for large ω . For (H5), the assumption $P_0(\lambda, \tau) \neq 0$ is automatically satisfied if $P_0(\lambda, \tau)$ is independent of τ , and its purpose is to write (2.1) in another equivalent form, i.e., (3.1) below, while $P_l(\lambda, \tau) \neq 0$, $l = 1, 2$, are presented to ensure the continuity and differentiability of the function $S_n^\pm(\omega, \tau)$, $n \in \mathbb{Z}$, defined in next section. The assumption (H6) is a technical assumption, and is prone to be true in most of applications. It will help to reduce the cases of graph for the function $S_n^\pm(\omega, \tau)$.

3. Crossing curves

This section is to determine all possible values of (τ, τ_1) such that (2.1) has purely imaginary roots. What makes the discussion in the following meaningful is the continuity of the zeros of the characteristic equation (2.1) with respect to the delay parameters (τ, τ_1) , that is, the following Rouché theorem.

Proposition 3.1. *As the delays (τ, τ_1) continuously vary within $I \times \mathbb{R}_+$, the number of zeros (counting multiplicity) of $D(\lambda; \tau, \tau_1)$ on \mathbb{C}_+ can change only if a zero appears on or cross the imaginary axis. Here \mathbb{C}_+ represents the right half complex plane.*

In the following we search the points $(\tau, \tau_1) \in I \times \mathbb{R}_+$ such that $\lambda = i\omega$, $\omega > 0$ is a zero of $D(\lambda, \tau, \tau_1)$. The curve, formed by all such those points, is referred to the “crossing curve” in the context. It is convenient to observe that, by (H5), $\lambda = i\omega$ is a characteristic root of $D(\lambda, \tau, \tau_1) = 0$ if and only if

$$1 + a_1(\omega, \tau)e^{-i\omega\tau} + a_2(\omega, \tau)e^{-i\omega\tau_1} = 0, \quad (3.1)$$

where

$$a_l(\omega, \tau) = P_l(i\omega, \tau)/P_0(i\omega, \tau), \quad l = 1, 2. \quad (3.2)$$

Proposition 3.2. *For $\omega > 0$, if $\lambda = i\omega$ is a zero of (3.1) for some $(\tau, \tau_1) \in I \times \mathbb{R}_+$, then (ω, τ) satisfies*

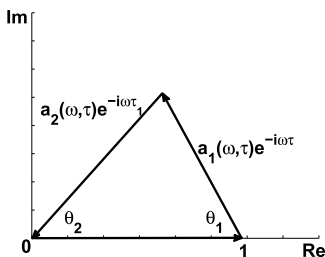


Fig. 1. Triangle formed by 1, $a_1(\omega, \tau)e^{-i\omega\tau}$, $a_2(\omega, \tau)e^{-i\omega\tau}$.

$$\begin{aligned}
 |a_1(\omega, \tau)| + |a_2(\omega, \tau)| &\geq 1, \\
 |a_1(\omega, \tau)| - |a_2(\omega, \tau)| &\leq 1, \\
 |a_2(\omega, \tau)| - |a_1(\omega, \tau)| &\leq 1.
 \end{aligned}
 \tag{3.3}$$

Proof. Equation (3.1) can be seen in the complex plane as Fig. 1. A triangle can be formed by three line segments with arbitrary orientation if and only if the length of any one side does not exceed the sum of the other two sides. \square

Inequalities (3.3) are equivalent to

$$\begin{aligned}
 F_1(\omega, \tau) &:= |P_1(i\omega, \tau)| + |P_2(i\omega, \tau)| - |P_0(i\omega, \tau)| \geq 0 \\
 F_2(\omega, \tau) &:= |P_1(i\omega, \tau)| - |P_2(i\omega, \tau)| - |P_0(i\omega, \tau)| \leq 0 \\
 F_3(\omega, \tau) &:= |P_2(i\omega, \tau)| - |P_1(i\omega, \tau)| - |P_0(i\omega, \tau)| \leq 0
 \end{aligned}
 \tag{3.4}$$

(3.3) or (3.4) determines the feasible region Ω for (ω, τ) , on which (3.1) may have solutions for τ_1 . The region Ω may be not connected in $\mathbb{R}_+ \times \mathbb{R}_+$, but it must be bounded in the direction of ω -axis. Indeed, by (H4), there exists an $\bar{\omega} > 0$ such that $F_1(\omega, \tau) < 0$ for all $\omega > \bar{\omega}$ and $\tau > 0$. This implies $\omega < \bar{\omega}$ as long as $(\omega, \tau) \in \Omega$. For each connected region Ω_k of Ω , the admissible range for ω is denoted by $I_k = [\omega_k^l, \omega_k^r]$, $k = 1, 2, \dots, N$. It should be pointed out that ω_k^l could be 0, and in this case, it follows from (H2) that I_k would become $(0, \omega_k^r]$. For each $\omega \in I_k$, there exist τ -intervals $I_\omega^k := [\tau_\omega^{k,l}, \tau_\omega^{k,r}] \subseteq I$, on which inequalities (3.3) or (3.4) hold. Moreover, $\tau_\omega^{k,l}$ could be 0 and $\tau_\omega^{k,r}$ could be $+\infty$. It is remarked that the interval I_ω^k may not be unique, when the region Ω_k is not convex. However, as will be seen, we find out that the interval I_ω^k for all the equations in the paper is uniquely determined for each fixed $\omega \in I_k$. When I_ω^k involves more than one interval, the discussions on the roots of $S_n^\pm(\omega, \tau) = 0$, given below, can be done for each subinterval of I_ω^k .

Let $\theta_1(\omega, \tau)$, $\theta_2(\omega, \tau)$ be the angles formed by 1 and $a_1(\omega, \tau)e^{-i\omega\tau}$, 1 and $a_2(\omega, \tau)e^{-i\omega\tau}$, respectively, as shown in Fig. 1. By the law of cosine, we have

$$\theta_1(\omega, \tau) = \arccos\left(\frac{1 + |a_1(\omega, \tau)|^2 - |a_2(\omega, \tau)|^2}{2|a_1(\omega, \tau)|}\right),
 \tag{3.5}$$

$$\theta_2(\omega, \tau) = \arccos\left(\frac{1 + |a_2(\omega, \tau)|^2 - |a_1(\omega, \tau)|^2}{2|a_2(\omega, \tau)|}\right).
 \tag{3.6}$$

For each fixed $\omega \in I_k$, we should note that $Im(a_1(\omega, \tau)e^{-i\omega\tau}) = 0$ if and only if $\theta_1(\omega, \tau) = 0$ or π , which is equivalent to $\tau = \tau_\omega^{k,l}$ or $\tau_\omega^{k,r}$. Hence, $Im(a_1(\omega, \tau)e^{-i\omega\tau})$ cannot change sign for $\tau \in \text{Int}I_\omega^k$. We consider the following two possible cases:

1) If $Im(a_1(\omega, \tau)e^{-i\omega\tau}) > 0$, then, from Fig. 1, we obtain:

$$\arg(a_1(\omega, \tau)e^{-i\omega\tau}) = \pi - \theta_1(\omega, \tau) \quad \text{and} \quad \arg(a_2(\omega, \tau)e^{-i\omega\tau_1}) = \theta_2(\omega, \tau) - \pi.$$

Therefore,

$$\arg(a_1(\omega, \tau)) - \omega\tau + 2n\pi = \pi - \theta_1(\omega, \tau), \quad \text{for some } n \in \mathbb{Z}, \quad (3.7)$$

and

$$\arg(a_2(\omega, \tau)) - \omega\tau_1 + 2j\pi = \theta_2(\omega, \tau) - \pi, \quad \text{for some } j \in \mathbb{Z}. \quad (3.8)$$

It follows from (3.8) that

$$\tau_1 = \frac{1}{\omega} [\arg(a_2(\omega, \tau)) - \theta_2(\omega, \tau) + (2j + 1)\pi], \quad j \in \mathbb{Z}. \quad (3.9)$$

2) If $Im(a_1(\omega, \tau)e^{-i\omega\tau}) < 0$, the triangular formed by 1, $a_1(\omega, \tau)e^{-i\omega\tau}$ and $a_2(\omega, \tau)e^{-i\omega\tau_1}$ is the mirror image of the one in Fig. 1 about the real axis. By a similar argument, we have

$$\arg(a_1(\omega, \tau)) - \omega\tau + 2n\pi = \pi + \theta_1(\omega, \tau), \quad \text{for some } n \in \mathbb{Z}, \quad (3.10)$$

and

$$\tau_1 = \frac{1}{\omega} [\arg(a_2(\omega, \tau)) + \theta_2(\omega, \tau) + (2j + 1)\pi], \quad \text{for some } j \in \mathbb{Z}. \quad (3.11)$$

It should be pointed out that n and j in (3.7), (3.9), (3.10) and (3.11) may depend on the values of ω and τ . From the above discussion, one can easily find the critical values of τ_1 according to (3.9) and (3.11), once the values of (ω, τ) satisfying (3.7) or (3.10) are determined. This motivates us to define the functions $S_n^\pm : \Omega \rightarrow \mathbb{R}$

$$S_n^\pm(\omega, \tau) = \tau - \frac{1}{\omega} [\arg(a_1(\omega, \tau)) + (2n - 1)\pi \pm \theta_1(\omega, \tau)], \quad n \in \mathbb{Z}. \quad (3.12)$$

Proposition 3.3. *If*

$$-\frac{P_1(i\omega; \tau)}{P_0(i\omega; \tau)} \notin \mathbb{R}_+ \quad (3.13)$$

for any $(\omega, \tau) \in \Omega$, then the functions $S_n^\pm(\omega, \tau)$, $n \in \mathbb{Z}$ are continuous and differentiable on Ω .

Proof. Suppose that Note that $a_1(\omega, \tau)$ and $a_2(\omega, \tau)$ are continuously differentiable on Ω_k . From (H5), it follows that the values of $|a_1(\omega, \tau)|$ and $|a_2(\omega, \tau)|$ can not be zero for any $(\omega, \tau) \in \Omega_k$. Therefore, $|a_1(\omega, \tau)|$ and $|a_2(\omega, \tau)|$ are also continuously differentiable on Ω_k , so is $\theta_1(\omega, \tau)$. It remains to show the continuity and differentiability of $\arg(a_1(\omega, \tau))$. Recall that the range of $\arg(a_1(\omega, \tau))$ is $(-\pi, \pi]$. Then, the points $(\omega', \tau') \in \Omega_k$ such that $\arg(a_1(\omega', \tau')) = \pi$ are the all discontinuities of $\arg(a_1(\omega, \tau))$. Therefore, it suffices to show that $\arg(a_1(\omega, \tau)) \neq \pi$ on Ω_k . Indeed, if $\arg(a_1(\omega', \tau')) = \pi$ for some (ω', τ') , then $-P_1(\omega', \tau')/P_0(\omega', \tau')$ must be a positive number, which is in contradiction with (3.13). \square

Remark 3.4. In practical applications, the assumption (3.13) can be removed. When (3.13) is violated, then for each fixed $n \in \mathbb{Z}$, $S_n^\pm(\omega, \tau)$ is discontinuous at $\{(\omega_0, \tau_0) : -a_1(\omega_0, \tau_0) \in \mathbb{R}_+\} \cap \Omega$. However, $S_n^\pm(\omega, \tau)$ will always be connected to $S_{n-1}^\pm(\omega, \tau)$ or $S_{n+1}^\pm(\omega, \tau)$ at these discontinuous points. Due to $\text{Im}\{a_1(\omega, \tau)\}$ and $\text{Re}\{a_1(\omega, \tau)\}$ are continuously differentiable functions on Ω , $\text{Im}\{a_1(\omega, \tau)\} = 0$ and $\text{Re}\{a_1(\omega, \tau)\} = 0$ can divide the feasible region Ω into several connected regions. Moreover, since $a_1(\omega, \tau) \neq 0$ for $(\omega, \tau) \in \Omega$, $\text{Im}\{a_1(\omega, \tau)\} = 0$ can not intersect with $\text{Re}\{a_1(\omega, \tau)\} = 0$ in the interior of Ω . Therefore, we can always define a new continuously differentiable function $\tilde{S}_n^\pm(\omega, \tau)$, by choosing appropriate $S_j^\pm(\omega, \tau)$ for j on each connected region, such that $\dots < \tilde{S}_n^+(\omega, \tau) < \tilde{S}_n^-(\omega, \tau) < \tilde{S}_{n+1}^+(\omega, \tau) < \dots$. Then, one can see all the results in these sections will remain valid if we replace $S_n^\pm(\omega, \tau)$ by $\tilde{S}_n^\pm(\omega, \tau)$ in the following discussion, when (3.13) does not hold.

If (3.12) has zeros for some $\omega \in I_k$, say $\hat{\tau}^{i\pm}(\omega)$, $i = 1, 2, \dots$, lying in I_ω^k , then we can set up the corresponding τ_1 value as follows:

$$\hat{\tau}_{1,i}^{j\pm}(\omega) = [\arg(a_2(\omega, \hat{\tau}^{i\pm})) + (2j^\pm + 1)\pi \mp \theta_2(\omega, \hat{\tau}^{i\pm})]/\omega, \tag{3.14}$$

for $j = j_0^\pm, j_0^\pm - 1, \dots$, where j_0^\pm are the smallest integers such that $\hat{\tau}_{1,i}^{j\pm}(\omega) > 0$. Now, the point $(\hat{\tau}^{i\pm}(\omega), \hat{\tau}_{1,i}^{j\pm}(\omega))$ will determine the values of τ and τ_1 , for which (2.1) has a pair of purely imaginary roots $\pm i\omega$. The set of all such points defines the crossing curves

$$\mathcal{T} = \{(\hat{\tau}^{i\pm}(\omega), \hat{\tau}_{1,i}^{j\pm}(\omega)) \in I \times \mathbb{R}_+ | \omega \in I_k, k = 1, 2, \dots, N\}. \tag{3.15}$$

Again, we underline that $i, j \in \mathbb{Z}$ must be compatible with positive (τ, τ_1) with $\tau \in I$.

Unlike the characteristic equation discussed in [5], it is observed from (3.12) that τ is implicitly determined by ω , and for any fixed ω , the roots of (3.12) for τ may only take at most finite values (depending on the function S_n^\pm and the shape of Ω). Therefore, it requires to examine more carefully about the geometric properties of $S_n^\pm(\omega, \tau)$ for finding the zeros of (3.12). Note that $\tau_\omega = \tau_\omega^{k,l} \neq 0$ or $\tau_\omega = \tau_\omega^{k,r} \neq +\infty$ must satisfy one of the following equations:

$$|a_1(\omega, \tau_\omega)| + |a_2(\omega, \tau_\omega)| = 1, \tag{3.16}$$

$$|a_1(\omega, \tau_\omega)| - |a_2(\omega, \tau_\omega)| = 1, \tag{3.17}$$

$$|a_2(\omega, \tau_\omega)| - |a_1(\omega, \tau_\omega)| = 1. \tag{3.18}$$

From (3.5) and (3.12), we have the following conclusions:

Please cite this article in press as: Q. An et al., Geometric stability switch criteria in delay differential equations with two delays and delay dependent parameters, J. Differential Equations (2018), <https://doi.org/10.1016/j.jde.2018.11.025>

Lemma 3.5.

- (1) If (3.16) or (3.17) is satisfied for $\tau_\omega = \tau_\omega^{k,l} \neq 0$ or $\tau_\omega = \tau_\omega^{k,r} \neq +\infty$, then $\theta_1(\omega, \tau_\omega) = 0$ and $S_n^+(\omega, \tau_\omega) = S_n^-(\omega, \tau_\omega)$ for this τ_ω .
- (2) If (3.18) is satisfied for $\tau_\omega = \tau_\omega^{k,l} \neq 0$ or $\tau_\omega = \tau_\omega^{k,r} \neq +\infty$, then $\theta_1(\omega, \tau_\omega) = \pi$ and $S_n^+(\omega, \tau_\omega) = S_{n+1}^-(\omega, \tau_\omega)$ for this τ_ω .

For each fixed $\omega \in I_k$, we can categorize the interval I_ω^k into four types, on which the graphs of $S_n^\pm(\omega, \tau)$ are different:

Type 1: $\theta_1(\omega, \tau_\omega^{k,l}) = \theta_1(\omega, \tau_\omega^{k,r})$.
 If $\theta_1(\omega, \tau_\omega^{k,l}) = \theta_1(\omega, \tau_\omega^{k,r}) = 0$, it then follows from Lemma 3.5 that $S_n^+(\omega, \tau)$ and $S_n^-(\omega, \tau)$ will form a sequence of closed curves for $\tau \in I_\omega^k, n \in \mathbb{Z}$. For the same reason, $S_n^+(\omega, \tau)$ and $S_{n+1}^-(\omega, \tau)$ will also form a sequence of closed curves when $\theta_1(\omega, \tau_\omega^{k,l}) = \theta_1(\omega, \tau_\omega^{k,r}) = \pi$. In either case, we can conclude that the number of zeros of (3.12), whenever exists, is even and finite.

Type 2: $\theta_1(\omega, \tau_\omega^{k,l}) \neq \theta_1(\omega, \tau_\omega^{k,r})$.
 If $\theta_1(\omega, \tau_\omega^{k,l}) = 0$ and $\theta_1(\omega, \tau_\omega^{k,r}) = \pi$, then $S_n^+(\omega, \tau_\omega^{k,l}) = S_n^-(\omega, \tau_\omega^{k,l})$ and $S_n^+(\omega, \tau_\omega^{k,r}) = S_{n+1}^-(\omega, \tau_\omega^{k,r})$. Therefore, the graphs of S_n^\pm for $n \in \mathbb{Z}$ will form an S-shaped curve, which extends infinitely along S_n -axis. Hence, (3.12) will always have zeros on I_ω^k . Applying a similar argument to the other case, i.e., $\theta_1(\omega, \tau_\omega^{k,l}) = \pi$ and $\theta_1(\omega, \tau_\omega^{k,r}) = 0$, one can still show the existence of zeros for (3.12) on I_ω^k .

Type 3: $\tau_\omega^{k,l} = 0$ and $\tau_\omega^{k,r} \neq +\infty$.
 The assumption (H6) implies that there exists a $\tilde{\tau}_\omega^{k,l} < 0$ such that the interval $I_\omega^k = [\tilde{\tau}_\omega^{k,l}, \tau_\omega^{k,r}]$ belongs to one of the above types. Then, the graph of S_n^\pm on $[\tilde{\tau}_\omega^{k,l}, \tau_\omega^{k,r}]$ could be either a sequence of closed curves or an S-shaped curve, as discussed above. However, we now only concentrate on finding zeros of S_n^\pm on $[0, \tau_\omega^{k,r}]$.

Type 4: $\tau_\omega^{k,r} = +\infty$.
 In this case, we claim that (3.12) will have infinite number of zeros on I_ω^k . In fact, since $\arg(a_1(\omega, \tau))$ and $\theta_1(\omega, \tau)$ are bounded for $(\omega, \tau) \in \Omega, \lim_{\tau \rightarrow +\infty} S_n^\pm(\omega, \tau) = \infty$ for any fixed n and ω . On the other hand, from the expression of S_n^\pm , we know that there exist $N \in \mathbb{Z}$ such that $S_n^\pm(\omega, \tau_\omega^{k,l}) < 0$ for $n > N$. Therefore, for fixed ω , the graph of $S_n^\pm(\omega, \tau)$ must intersect with τ -axis for $\tau \in (\tau_\omega^{k,l}, +\infty)$ for $n > N$, that is, there are infinite number of admissible values for τ corresponding to this fixed ω .

Accordingly, we can also divide each connected component Ω_k of Ω into four disjoint parts $\Omega_{ki}, i = 1, 2, 3, 4$, such that on Ω_{ki} , the interval I_ω^k is Type i for each fixed ω . These four types of I_ω^k are illustrated by the following Example.

Example 3.6. Consider (2.1) with

$$P_0(\lambda, \tau) = \lambda + 1, \quad P_1(\lambda, \tau) = 5e^{-\tau} - 0.5, \quad P_2(\lambda, \tau) = 2.$$

The feasible region Ω , which is enclosed by $\sum_{k=0}^2 |P_k(i\omega, \tau)| - 2|P_l(i\omega, \tau)| = 0, l = 0, 1, 2, \omega$ -axis and τ -axis, is shown in Fig. 2. There are two connected subregions Ω_1 and Ω_2 , which deter-

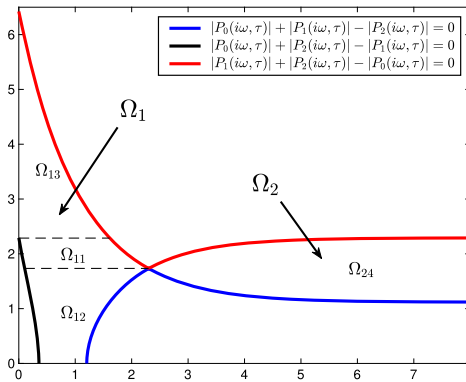


Fig. 2. Feasible region Ω for (ω, τ) in Example 3.6. (For interpretation of the colors in the figure(s), the reader is referred to the web version of this article.)

mines two admissible ranges of ω : $I_1 = (0, 6.423]$ and $I_2 = [1.119, 2.291]$. In addition, Ω_1 is partitioned into three regions Ω_{11} , Ω_{12} and Ω_{13} , according to the different types of intervals I_ω^k . The zeros of S_n^\pm on I_ω^k can be summarized as followed:

- When $(\omega, \tau) \in \Omega_{11}$, I_ω^1 is of Type 1. For fixed ω , (3.12) has two zeros, as shown in Fig. 3(a).
- When $(\omega, \tau) \in \Omega_{12}$, I_ω^1 is of Type 2. In this case, (3.12) only has one zero for each ω , see Fig. 3(b).
- When $(\omega, \tau) \in \Omega_{13}$, I_ω^1 is of Type 3. The graphs of S_n^\pm also form a sequence of loops on $[\tilde{\tau}_\omega^{1,l}, \tau_\omega^{1,r}]$. However, they may not intersect τ -axis, see Fig. 3(c).
- When $(\omega, \tau) \in \Omega_{24}$, I_ω^2 is of Type 4 and (3.12) have infinite number of zeros for each ω , see Fig. 3(d).

If ω takes the values throughout the interval I_k , $k = 1, 2, \dots$, then we can get the curve $\mathcal{C} := \{(\omega, \hat{\tau}^\pm(\omega)) : \omega \in I_k, S_n^\pm(\omega, \hat{\tau}^\pm(\omega)) = 0, k = 1, 2, \dots, n \in \mathbb{Z}\}$ on Ω , which will determine the crossing curves on (τ, τ_1) -plane. The curve \mathcal{C} might consist of several components, such that on each component, τ is a function of ω . Now, we claim that every such component of the curve must touch the boundary of Ω_k at the end points under further assumptions. Note that the boundary of Ω_k may include part of τ -axis. However, by (H2), every component of \mathcal{C} will not touch τ -axis.

Lemma 3.7. Assume that $S_n^\pm(\omega, \tau)$ has a zero root lies in $\text{int } \Omega$ for some n , say (ω_0, τ_0) , and satisfies $\partial_\tau S_n^\pm(\omega_0, \tau_0) \neq 0$. Then there exist intervals I_ω, I_τ containing ω_0 and τ_0 , respectively, and a continuously differentiable function $\hat{\tau}^{i\pm} : I_\omega \subset \mathbb{R}_+ \rightarrow I_\tau$ such that $\hat{\tau}^{i\pm}(\omega_0) = \tau_0$ and $S_i^\pm(\omega, \hat{\tau}^{i\pm}(\omega)) = 0$. Moreover, the endpoints of the curve $(\omega, \hat{\tau}^{i\pm}(\omega))$ are either connect to the boundary of Ω or the point $(\bar{\omega}, \bar{\tau}) \in \text{int } \Omega$ that satisfies $\hat{\tau}^{i\pm}(\bar{\omega}) = \bar{\tau}$ and $\partial_\tau S_i^\pm(\bar{\omega}, \bar{\tau}) = 0$.

Proof. Since $S_n^\pm(\omega, \tau)$ is a continuously differentiable function of $(\omega, \tau) \in \Omega$, the implicit function theorem indicates that there exist neighborhoods $U(\omega_0)$ of ω_0 , $U(\tau_0)$ of τ_0 and a unique continuously differentiable function $\hat{\tau}^{i\pm} : U(\omega_0) \rightarrow U(\tau_0)$ such that $\hat{\tau}^{i\pm}(\omega_0) = \tau_0$ and $S_n^\pm(\omega, \hat{\tau}^{i\pm}(\omega)) = 0$ for all $\omega \in U(\omega_0)$. Suppose that $(\omega', \hat{\tau}^{i\pm}(\omega')) \in \text{int } \Omega$ is an endpoint of $(\omega, \hat{\tau}^{i\pm}(\omega))$ and satisfies $\partial_\tau S_n^\pm(\omega', \hat{\tau}^{i\pm}(\omega')) \neq 0$. Then, the function $\hat{\tau}^{i\pm}(\omega)$ can be extended to

Please cite this article in press as: Q. An et al., Geometric stability switch criteria in delay differential equations with two delays and delay dependent parameters, J. Differential Equations (2018), <https://doi.org/10.1016/j.jde.2018.11.025>

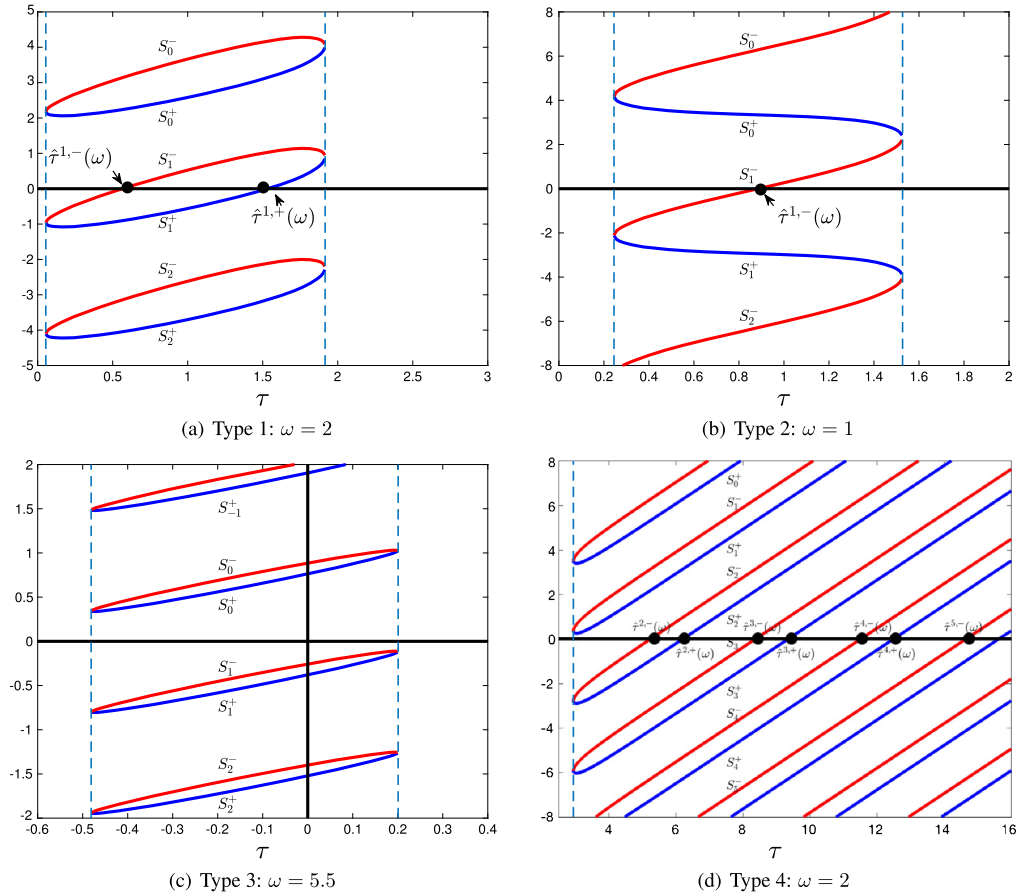


Fig. 3. The graphs of $S_n^\pm(\omega, \tau)$ for different types of intervals I_ω^k in Example 3.6.

a larger domain. This process can be repeated until this curve reaches the boundary of Ω or another $(\bar{\omega}, \bar{\tau}) \in \text{int } \Omega$ such that $\partial_\tau S_i^\pm(\bar{\omega}, \bar{\tau}) = 0$. \square

In the rest of this section, we further assume that

(H7) $\partial_\tau S_n^\pm(\omega, \tau) \neq 0$ for any $(\omega, \tau) \in \mathcal{C}$.

By (H7) and Lemma 3.7, the endpoints of every component of \mathcal{C} , say $(\omega_e, \hat{\tau}^{i\pm}(\omega_e))$, must lie on the boundary of Ω and can be divided into four types:

Type A: (3.16) is satisfied for $(\omega, \tau_\omega) = (\omega_e, \hat{\tau}^{i\pm}(\omega_e))$.

In this case, $\theta_1 = 0, \theta_2 = 0$. The curves $(\omega, \hat{\tau}^{i\pm}(\omega))$, if both exist, then it follows that $(\hat{\tau}^{i+}(\omega_e), \hat{\tau}_{1,i}^{j+}(\omega_e)) = (\hat{\tau}^{i-}(\omega_e), \hat{\tau}_{1,i}^{j-}(\omega_e))$.

Type B: (3.17) is satisfied for $(\omega, \tau_\omega) = (\omega_e, \hat{\tau}^{i\pm}(\omega_e))$.

In this case, $\theta_1 = 0, \theta_2 = \pi$. The curves $(\omega, \hat{\tau}^{i\pm}(\omega))$, if both exist, then it follows that $(\hat{\tau}^{i+}(\omega_e), \hat{\tau}_{1,i}^{j+}(\omega_e)) = (\hat{\tau}^{i-}(\omega_e), \hat{\tau}_{1,i}^{(j-1)-}(\omega_e))$.

Type C: (3.18) is satisfied for $(\omega, \tau_\omega) = (\omega_e, \hat{\tau}^{i\pm}(\omega_e))$.

In this case, $\theta_1 = \pi, \theta_2 = 0$. The curves $(\omega, \hat{\tau}^{i+}(\omega))$ and $(\omega, \hat{\tau}^{(i+1)-}(\omega))$, if both exist, then it follows that $(\hat{\tau}^{i+}(\omega_e), \hat{\tau}_{1,i}^{j+}(\omega_e)) = (\hat{\tau}^{(i+1)-}(\omega_e), \hat{\tau}_{1,i+1}^{j-}(\omega_e))$.

Type D: $\hat{\tau}^{i\pm}(\omega_e) = 0$.

In this case, the curve $(\omega, \hat{\tau}^{i\pm}(\omega_e))$ can be extended to the outside of the feasible region Ω and eventually arrive at a point that belongs to one of the above types.

Again, if we regard Type D as one of other three Types on the “extended” feasible region Ω , then each component (on which, τ is a function of ω) of curve \mathcal{C} falls into the following six categories, based on the type of its end points: Type AA, Type BB, Type CC, Type AB, Type AC, Type BC. (For instant, Type AA indicates that both end points of the component are Type A.)

Proposition 3.8. *Assume that (H7) holds. Then, any two components of \mathcal{C} will not intersect in $\text{Int } \Omega$.*

Proof. Suppose there are two components, denoted by $\mathcal{P}_1 := \{(\omega, \bar{\tau}(\omega)), \omega \in J_1\}$ and $\mathcal{P}_2 := \{(\omega, \tilde{\tau}(\omega)), \omega \in J_2\}$, respectively, intersect at an interior point of Ω , say $(\omega^*, \tau(\omega^*))$. Due to $\dots < S_n^+(\omega, \tau) < S_n^-(\omega, \tau) < S_{n-1}^+(\omega, \tau) < \dots$, for $(\omega, \tau) \in \text{Int } \Omega$, it follows that $\mathcal{P}_1, \mathcal{P}_2$ must be the zeros of a same function, say $S_{n^*}^\pm$. Therefore, either $\mathcal{P}_1 = \mathcal{P}_2$ in $\text{Int } \Omega$ or there is a ω_* such that $(\omega_*, \bar{\tau}(\omega_*)) = (\omega_*, \tilde{\tau}(\omega_*))$ and $(\omega, \bar{\tau}(\omega)) \neq (\omega, \tilde{\tau}(\omega))$ for some ω sufficiently close to ω_* . We claim the latter is absurd. In fact, since $\partial_\tau S_n^\pm(\omega_*, \tau(\omega_*)) \neq 0$, it follows from the implicit function theorem that the implicit function $\hat{\tau}^{n^*\pm}(\omega)$ in the neighborhood of ω_* is unique. \square

The component of \mathcal{C} may be isolated, i.e., it has no intersections with the other ones. Other than that, it is possible that the components of \mathcal{C} are connected at the endpoints (by Proposition 3.8) in the following four manners:

- (a): One component is connected to another one at one of its endpoints, that is, these two components form a V-shaped (also open-ended) curve in Ω ;
- (b): Two components are connected at both ends, forming a closed loop in Ω ;
- (c): No less than three components are connected end to end, forming an open-ended curve on Ω ;
- (d): No less than three components are connected end to end, forming a closed curve on Ω .

The curves, composed of the components of \mathcal{C} in either case of (a)–(d), are said to be connected segments in this context. Based on the above classification of connected segment, we can see that the shape of each connected segment essentially has two forms: open-ended and looped. For looped connected segment, we will show that (d) can not occur, relying on the following two lemmas.

Lemma 3.9. *If there exists a component of Type AC or BC in the connected segment, formed by no less than three components, then this connected segments must be open-ended (can not be closed).*

Proof. We only show the assertion for Type AC. Without loss of generality, let $(\omega, \hat{\tau}^{i+}(\omega))$ be the component of Type AC. From (3.12), it follows that $(\omega, \hat{\tau}^{i+}(\omega))$ can only connect to

Please cite this article in press as: Q. An et al., Geometric stability switch criteria in delay differential equations with two delays and delay dependent parameters, J. Differential Equations (2018), <https://doi.org/10.1016/j.jde.2018.11.025>

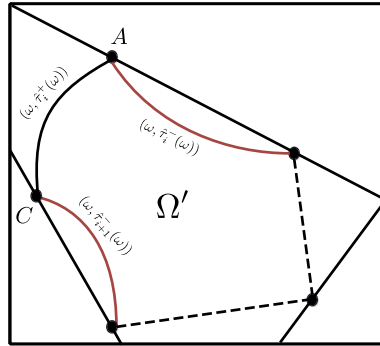


Fig. 4. $(\omega, \hat{\tau}^{i-}(\omega))$ and $(\omega, \hat{\tau}^{(i+1)-}(\omega))$ are lying on the same side of $(\omega, \hat{\tau}^{i+}(\omega))$.

$(\omega, \hat{\tau}^{i-}(\omega))$ at the endpoint of Type A, and $(\omega, \hat{\tau}^{(i+1)-}(\omega))$ at the endpoint of Type C. If these two components $(\omega, \hat{\tau}^{i-}(\omega))$ and $(\omega, \hat{\tau}^{(i+1)-}(\omega))$ lie on the different sides of $(\omega, \hat{\tau}^{i+}(\omega))$. Then, according to Proposition 3.8, the connected segment involving $(\omega, \hat{\tau}^{i+}(\omega))$ must form an open ended curve in Ω .

If $(\omega, \hat{\tau}^{i-}(\omega))$ and $(\omega, \hat{\tau}^{(i+1)-}(\omega))$ are lying on the same side of $(\omega, \hat{\tau}^{i+}(\omega))$. We suppose that these three components can form a closed curve together with additional components, as shown in Fig. 4. Then, this closed curve determines a region $\Omega' \subset \Omega$, on which S_i^\pm and S_{i+1}^\pm do not change signs. From the monotonicity of $S_n^\pm(\omega, \tau)$, we obtain $S_i^+(\omega, \hat{\tau}^{i-}(\omega)) < S_i^+(\omega, \hat{\tau}^i(\omega)) = 0$. Then, $0 > S_i^+(\omega, \hat{\tau}^{(i+1)-}(\omega)) > S_{i+1}^-(\omega, \hat{\tau}^{(i+1)-}(\omega)) = 0$, which is a contradiction. \square

Lemma 3.10. *If the connect segment consists of no less than three components \mathcal{C} , then it must be open-ended.*

Proof. Suppose that there is a looped connected segment Λ of \mathcal{C} containing three or more components. It then follows from Lemma 3.9 that there is no component of Type AC or BC included in Λ . Therefore, either each component of Λ belongs to one of Type AA, BB, AB, or all the components of Λ belong to Type CC.

Recall that $(\omega, \hat{\tau}^{i+}(\omega))$ can only connect to $(\omega, \hat{\tau}^i(\omega))$ at the endpoint of Type A or B, and $(\omega, \hat{\tau}^{(i+1)-}(\omega))$ at the endpoint of Type C. Then, Λ is composed by either $\{(\omega, \hat{\tau}^{\pm}(\omega))\}$ or $\{(\omega, \hat{\tau}^{i+}(\omega)), (\omega, \hat{\tau}^{(i+1)-}(\omega))\}$ for a fixed $i \in \mathbb{N}$. However, for any case, there must exists an endpoint of these components, say $(\omega_e, \tau(\omega_e))$, and a function S_i^+ or S_i^- , such that $S_i^+(\omega_e, \tau(\omega_e)) = S_i^+(\omega_e, \hat{\tau}^{i+}(\omega_e)) = 0$ or $S_i^-(\omega_e, \tau(\omega_e)) = S_i^-(\omega_e, \hat{\tau}^i(\omega_e)) = 0$, with $\tau(\omega_e) \neq \hat{\tau}^{\pm}(\omega_e)$, see Fig. 5. It is in contradiction with (H7). Therefore, Λ must be open-ended in Ω . \square

As a consequence of Lemma 3.9 and Lemma 3.10, we have the following conclusion on looped connected segment.

Proposition 3.11. *The looped connected segment in Ω , whenever exists, must be formed by two components of \mathcal{C} in the same type AA, BB, CC or AB,*

Now, we are ready to show the shape of crossing curves, associated with different type of connected segments of \mathcal{C} .

Please cite this article in press as: Q. An et al., Geometric stability switch criteria in delay differential equations with two delays and delay dependent parameters, J. Differential Equations (2018), <https://doi.org/10.1016/j.jde.2018.11.025>

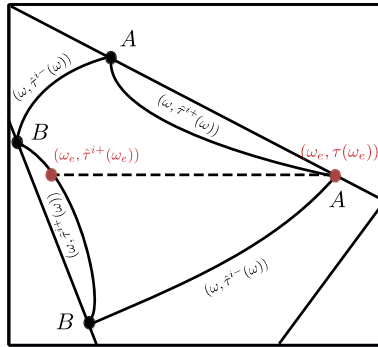


Fig. 5. A closed curve in Ω consists of four components of C .

Proposition 3.12. *For the open-ended connected segment, which may consist of one or several components of C , if it is bounded, then the associated crossing curve on (τ, τ_1) -plane are a series of open ended curves oriented along the τ_1 -axis, which is bounded in the direction of τ -axis. Otherwise, the associated crossing curves on (τ, τ_1) -plane are a series of spiral-like curves or open ended curves along the τ_1 -axis, and each of these curves approaching ∞ in the direction of τ -axis.*

Proof. Suppose that Γ_1 and Γ_2 are two components in an open-ended connected segment, which intersect at one endpoint, say (ω_e, τ_e) , of Type A. Then, the associated crossing curves, denoted by $(\hat{\tau}^{i+}(\omega), \hat{\tau}_{1,i}^{j+}(\omega))$ and $(\hat{\tau}^{i-}(\omega), \hat{\tau}_{1,i}^{j-}(\omega))$ are connected at $\omega = \omega_e$, forming continuous curves in (τ, τ_1) -plane. For Type B and C, $(\hat{\tau}^{i+}(\omega), \hat{\tau}_{1,i}^{j+}(\omega))$ will connect $(\hat{\tau}^{i-}(\omega), \hat{\tau}_{1,i}^{(j-1)-}(\omega))$ and $(\hat{\tau}^{(i+1)-}(\omega), \hat{\tau}_{1,i}^{j-}(\omega))$ at $\omega = \omega_e$. Repeating this process to the other components (if exists), we will obtain an open-ended crossing curve.

Furthermore, if the open-ended connected segment is bounded, then it must consist of only finite components of C . Hence, a series of open-ended crossing curve can be extended along τ_1 axis, by increasing j . Otherwise, the connected segment must be unbounded in the direction of τ -axis. This implies the admissible value for τ can reach ∞ . If the connected segment is composed by infinity many components, then according to Proposition 3.8 and assumption (H4), it must be a wavy line on (ω, τ) -plane. Therefore, the process discussed in the preceding paragraph will be repeated indefinitely. Then, by increasing the index j , a series of spiral-like crossing curves spread out in the direction of τ -axis but not necessarily parallel to τ -axis will be obtained. If the connected segment contains finitely many components, then a series of open ended crossing curves with the values of τ approaching ∞ will be formed. \square

Proposition 3.13. *For the looped connected segment, the associated crossing curves on (τ, τ_1) -plane are either a series of closed curves or a spiral-like curve oriented along the τ_1 -axis.*

Proof. Suppose that the two components in looped connected segment are both Type AA. Without loss of generality, let $\Gamma_1 := (\omega, \hat{\tau}^{i+}(\omega))$ be one of these components, and the associated crossing curve is denoted by $\Theta_1 := (\hat{\tau}^{i+}(\omega), \hat{\tau}_{1,i}^{j+}(\omega))$. It is easy to known that the other components is $\Gamma_2 := (\omega, \hat{\tau}^{i-}(\omega))$ and the associated crossing curve is given by

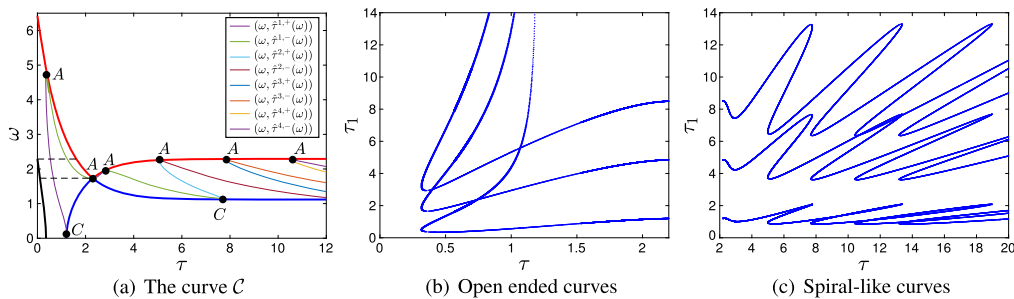


Fig. 6. The curve \mathcal{C} and the crossing curves \mathcal{T} for Example 3.6.

$\Theta_2 := (\hat{\tau}^{i-}(\omega), \hat{\tau}_{1,i}^{j-}(\omega))$. Since the endpoints, say $(\omega_e, \hat{\tau}^{i\pm}(\omega_e))$, are of Type A, it follows that $\theta_1(\omega_e, \hat{\tau}^{i\pm}(\omega_e)) = 0$ and $\theta_2(\omega_e, \hat{\tau}^{i\pm}(\omega_e)) = 0$. From (3.14), we have $\hat{\tau}_{1,i}^{j+}(\omega_e) = (\omega_e, \hat{\tau}_{1,i}^{j-}(\omega_e))$. Therefore, Θ_1 and Θ_2 are connected at both ends, enclosing a closed curve on (τ, τ_1) -plane. Moreover, this closed curve can be extended along τ_1 -axis by increasing the index j . The proof for Type BB and CC is analogous as above, while the crossing curve Θ_1 is connected to $(\hat{\tau}^{i-}(\omega), \hat{\tau}_{1,i}^{(j-1)-}(\omega))$ and $(\hat{\tau}^{(i+1)-}(\omega), \hat{\tau}_{1,(i+1)}^{j-}(\omega))$, respectively.

If the connected components are both Type AB, Θ_1 is connected to $(\hat{\tau}^{i-}(\omega), \hat{\tau}_{1,i}^{j-}(\omega))$ and $(\hat{\tau}^{i-}(\omega), \hat{\tau}_{1,i}^{(j-1)-}(\omega))$ at its ends, respectively. By increasing j again, we will have a spiral-like curve oriented along τ_1 -axis. \square

Now, we have the following description of crossing curves for (2.1).

Theorem 3.14. Under the assumptions (H1) – (H7), the crossing curve on (τ, τ_1) -plane consists of one or several curves in the following categories:

- (I) A series of open ended curves oriented along τ_1 -axis;
- (II) A series of closed curves oriented along τ_1 -axis;
- (III) A spiral-like curve spreading out along τ_1 -axis;
- (IV) A series of spiral-like curves oriented along τ_1 -axis, and each of these curves approaching ∞ in the direction of τ -axis;
- (V) Truncated curves of one of the above three cases.

Remark 3.15. The truncation of a series of closed curves or open ended curves are a sequence of open ended curves. However, in the case of spiral-like curve extended indefinitely along τ_1 -axis, the truncated curve might have complex structure.

Example 3.16. Choose $P_0(\lambda, \tau), P_1(\lambda, \tau), P_2(\lambda, \tau)$ as in Example 3.6. For each $\omega \in I_1$ and $\omega \in I_2$, identify the zeros of (3.12). Then, we can obtain the curve \mathcal{C} on Ω , see Fig. 6(a). It is observed that \mathcal{C} is composed by a bounded open-ended segment on Ω_1 and a unbounded open-ended segment that is formed by one curve of Type A and infinite curves of Type AC, in the manner of (c), on Ω_2 . It follows from Proposition 3.12 that the crossing curves are consist of a branch of open ended curves (see Fig. 6(b)), and a sequence of spiral-like curve that spreads out along τ -axis (see Fig. 6(c)).

For other types of crossing curves, please refer to Appendix A.

4. Crossing directions

Assume that $(\tau^*, \tau_1^*) \in \mathcal{T}$, then there is an $\omega^* > 0$ such that $(i\omega^*, \tau^*, \tau_1^*)$ is a zero of the characteristic equation (2.1). If $\frac{\partial D}{\partial \lambda}(i\omega^*, \tau^*, \tau_1^*) \neq 0$, then denote by $\lambda(\tau, \tau_1) = \alpha(\tau, \tau_1) + i\omega(\tau, \tau_1)$ the simple root of (2.1), in the neighborhood of (τ^*, τ_1^*) , which satisfies $\alpha(\tau^*, \tau_1^*) = 0$ and $\omega(\tau^*, \tau_1^*) = \omega^*$. In this section, we will discuss the direction of $\lambda(\tau, \tau_1)$ crossing the imaginary axis, as (τ, τ_1) deviates from (τ^*, τ_1^*) along a certain direction. As in [5,17], we call the direction of the crossing curve \mathcal{T} that corresponds to increasing ω the *positive direction*, and the region on the left-hand (right-hand) side when we move along the positive direction of the curve *the region on the left (right)*.

For the sake of convenience, let

$$\begin{aligned} R_0(\tau, \tau_1) &= \operatorname{Re} \left\{ \frac{\partial D(\lambda, \tau, \tau_1)}{\partial \lambda} \right\}, & I_0(\tau, \tau_1) &= \operatorname{Im} \left\{ \frac{\partial D(\lambda, \tau, \tau_1)}{\partial \lambda} \right\}, \\ R(\tau, \tau_1) &= \operatorname{Re} \left\{ \frac{\partial D(\lambda, \tau, \tau_1)}{\partial \tau} \right\}, & I(\tau, \tau_1) &= \operatorname{Im} \left\{ \frac{\partial D(\lambda, \tau, \tau_1)}{\partial \tau} \right\}, \\ R_1(\tau, \tau_1) &= \operatorname{Re} \left\{ \frac{\partial D(\lambda, \tau, \tau_1)}{\partial \tau_1} \right\}, & I_1(\tau, \tau_1) &= \operatorname{Im} \left\{ \frac{\partial D(\lambda, \tau, \tau_1)}{\partial \tau_1} \right\}. \end{aligned} \tag{4.1}$$

Since $R_0(\tau^*, \tau_1^*)^2 + I_0(\tau^*, \tau_1^*)^2 \neq 0$, we have

$$\begin{pmatrix} \frac{\partial \alpha}{\partial \tau} & \frac{\partial \alpha}{\partial \tau_1} \\ \frac{\partial \omega}{\partial \tau} & \frac{\partial \omega}{\partial \tau_1} \end{pmatrix} = - \begin{pmatrix} R_0(\tau, \tau_1) & -I_0(\tau, \tau_1) \\ I_0(\tau, \tau_1) & R_0(\tau, \tau_1) \end{pmatrix}^{-1} \begin{pmatrix} R(\tau, \tau_1) & R_1(\tau, \tau_1) \\ I(\tau, \tau_1) & I_1(\tau, \tau_1) \end{pmatrix} \tag{4.2}$$

On the other hand, if $R_1(\tau^*, \tau_1^*)I(\tau^*, \tau_1^*) - R(\tau^*, \tau_1^*)I_1(\tau^*, \tau_1^*) \neq 0$, the implicit theorem indicates that τ and τ_1 can be regard as a function of α and ω at a neighborhood of $(0, \omega^*)$. Then we obtain

$$\begin{pmatrix} \frac{\partial \tau}{\partial \alpha} & \frac{\partial \tau}{\partial \omega} \\ \frac{\partial \tau_1}{\partial \alpha} & \frac{\partial \tau_1}{\partial \omega} \end{pmatrix} = - \begin{pmatrix} R(\tau, \tau_1) & R_1(\tau, \tau_1) \\ I(\tau, \tau_1) & I_1(\tau, \tau_1) \end{pmatrix}^{-1} \begin{pmatrix} R_0(\tau, \tau_1) & -I_0(\tau, \tau_1) \\ I_0(\tau, \tau_1) & R_0(\tau, \tau_1) \end{pmatrix}. \tag{4.3}$$

A careful calculation gives that

$$\left(\frac{\partial \alpha}{\partial \tau}, \frac{\partial \alpha}{\partial \tau_1} \right) = \frac{R(\tau, \tau_1)I_1(\tau, \tau_1) - R_1(\tau, \tau_1)I(\tau, \tau_1)}{R_0(\tau, \tau_1)^2 + I_0(\tau, \tau_1)^2} \left(\frac{\partial \tau_1}{\partial \omega}, -\frac{\partial \tau}{\partial \omega} \right)$$

Due to $(\partial \tau_1 / \partial \omega, -\partial \tau / \partial \omega)$ is the normal vector of the crossing curve Γ pointing to the right region, we can conclude that if

$$R(\tau, \tau_1)I_1(\tau, \tau_1) - R_1(\tau, \tau_1)I(\tau, \tau_1) > 0, \tag{4.4}$$

Please cite this article in press as: Q. An et al., Geometric stability switch criteria in delay differential equations with two delays and delay dependent parameters, J. Differential Equations (2018), <https://doi.org/10.1016/j.jde.2018.11.025>

the pair of eigenvalues $\alpha(\tau, \tau_1) \pm i\omega(\tau, \tau_1)$ of the characteristic equation (2.1) cross the imaginary axis to the right half of the complex plane when (τ, τ_1) crosses the crossing curve to the region on the right. And the crossing is in the opposite direction if the inequality is reversed. This allows us to get the following theorem.

Theorem 4.1. *The characteristic equation (2.1) admits a pair of conjugate roots $\pm i\omega^*$, for $(\tau, \tau_1) = (\tau^*, \tau_1^*) \in \mathcal{T}$. If $\frac{\partial D}{\partial \lambda}(i\omega^*, \tau^*, \tau_1^*) \neq 0$, then (2.1) has a pair of conjugate complex roots $\lambda^\pm(\tau, \tau_1) = \alpha(\tau, \tau_1) \pm i\omega(\tau, \tau_1)$ in some neighborhood of (τ^*, τ_1^*) , such that $\alpha(\tau^*, \tau_1^*) = 0$ and $\omega(\tau^*, \tau_1^*) = \omega^*$. Furthermore, $\lambda^\pm(\tau, \tau_1)$ cross the imaginary axis from left to right, as (τ, τ_1) passes through the crossing curve to the region on the right (left) whenever $\delta(\tau^*, \tau_1^*) > 0$ ($\delta(\tau^*, \tau_1^*) < 0$), where*

$$\delta(\tau^*, \tau_1^*) = -\operatorname{Re} \left\{ \left[P_{0\tau}^* e^{i\omega^* \tau_1^*} + (P_{1\tau}^* - i\omega^* P_1^*) e^{i\omega^* (\tau_1^* - \tau^*)} + P_{2\tau}^* \right] \overline{P_2^*} \right\} \quad (4.5)$$

with $P_l^* = P_l(i\omega^*, \tau^*)$ and $P_{l\tau}^* = \frac{\partial P_l}{\partial \tau}(i\omega^*, \tau^*)$, $l = 0, 1, 2$.

Proof. We just need to proof (4.5). Since

$$R(\tau^*, \tau_1^*) I_1(\tau^*, \tau_1^*) - R_1(\tau^*, \tau_1^*) I(\tau^*, \tau_1^*) = -\operatorname{Im} \left\{ \frac{\partial D}{\partial \tau}(i\omega^*, \tau^*, \tau_1^*) \cdot \overline{\frac{\partial D}{\partial \tau_1}(i\omega^*, \tau^*, \tau_1^*)} \right\},$$

a direct calculation gives that

$$\begin{aligned} & R(\tau^*, \tau_1^*) I_1(\tau^*, \tau_1^*) - R_1(\tau^*, \tau_1^*) I(\tau^*, \tau_1^*) \\ &= -\omega^* \operatorname{Re} \left\{ \left[P_{0\tau}^* e^{i\omega^* \tau_1^*} + (P_{1\tau}^* - i\omega^* P_1^*) e^{i\omega^* (\tau_1^* - \tau^*)} + P_{2\tau}^* \right] \overline{P_2^*} \right\}, \end{aligned}$$

which completes the proof. \square

Example 4.2. Consider again the characteristic equation in Example 3.6, the crossing curve \mathcal{T} of which has been found in Example 3.16. For any $(\tau^*, \tau_1^*) \in \mathcal{T}$, according to Theorem 4.1, we have

$$\delta(\tau^*, \tau_1^*) = \operatorname{Re} \left\{ [5e^{-\tau^*} + i\omega^* (5e^{-\tau^*} - 0.5)] e^{i\omega^* (\tau_1^* - \tau^*)} \right\}. \quad (4.6)$$

Then, the crossing directions of \mathcal{T} are obtained. In Fig. 7, we show that the characteristic roots $\lambda^\pm(\tau, \tau_1)$ cross the imaginary axis from left to right as (τ, τ_1) pass through \mathcal{T} along the directions of the arrow.

5. An epidemic model

It should be pointed out that the geometric method present in this context is also applicable to other characteristic equations, such as:

$$D(\lambda, \tau, \tau_1) := P_0(\lambda, \tau) + P_1(\lambda, \tau) e^{-\lambda \tau_1} + P_2(\lambda, \tau) e^{-\lambda(\tau + \tau_1)} = 0. \quad (5.1)$$

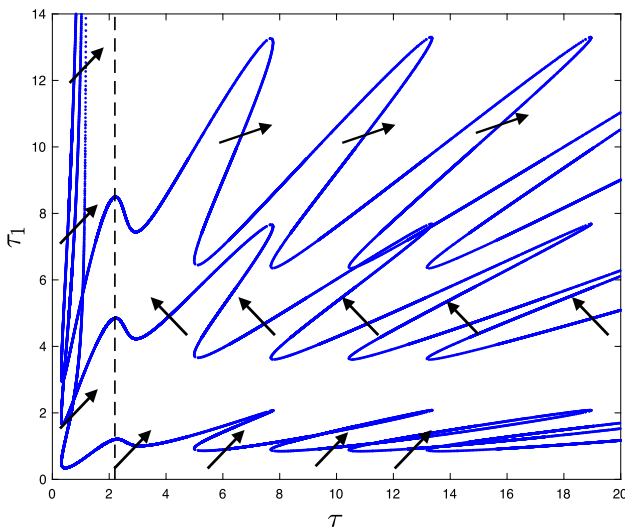


Fig. 7. The crossing directions of \mathcal{T} for Example 3.6. The crossing curves are from Fig. 6(b) and 6(c), which is separated by black-dotted line.

We shall illustrate this process by the following epidemic model.

$$\begin{cases} S'(t) = bS(t)(1 - S(t)) - \beta e^{-m\tau_1} S(t)I(t - \tau_1) \\ I'(t) = \beta e^{-m\tau_1} S(t)I(t - \tau_1) - \beta e^{-d\tau} S(t - \tau)I(t - \tau_1 - \tau) - dI(t) \\ R'(t) = \beta e^{-d\tau} S(t - \tau)I(t - \tau_1 - \tau) - dR(t) \end{cases} \quad (5.2)$$

Here, S , I and R denotes the population of susceptible, infected and recovered population, respectively; b and d represent the birth and death rate; β is the infection coefficient; τ_1 is the latent period; τ is the period from infection to recovery. The dynamics of (5.2) are determined by the first two equations, i.e.,

$$\begin{cases} S'(t) = bS(t)(1 - S(t)) - \beta e^{-m\tau_1} S(t)I(t - \tau_1) \\ I'(t) = \beta e^{-m\tau_1} S(t)I(t - \tau_1) - \beta e^{-d\tau} S(t - \tau)I(t - \tau_1 - \tau) - dI(t) \end{cases} \quad (5.3)$$

In a first attempt, we consider that m is sufficiently small, that is, $e^{-m\tau_1}$ is almost 1. Hence, the system becomes:

$$\begin{cases} S'(t) = bS(t)(1 - S(t)) - \beta S(t)I(t - \tau_1) \\ I'(t) = \beta S(t)I(t - \tau_1) - \beta e^{-d\tau} S(t - \tau)I(t - \tau_1 - \tau) - dI(t) \end{cases} \quad (5.4)$$

For (5.4), there are three steady states: $E_0 = (0, 0)$, $E_{+0} = (1, 0)$ and $E_{++} = (S^*(\tau), I^*(\tau))$, where

$$S^*(\tau) = \frac{d}{\beta(1 - e^{-d\tau})} > 0, \quad I^*(\tau) = \frac{b[1 - S^*(\tau)]}{\beta} = \frac{b}{\beta} \left[1 - \frac{d}{\beta(1 - e^{-d\tau})} \right].$$

Moreover, $I^*(\tau) > 0$ if and only if $\beta > d$ and $\tau > \frac{1}{d} \log \frac{\beta}{\beta - d} := \tau^*$.

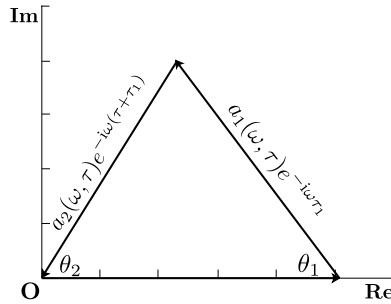


Fig. 8. Triangle formed by $1, a_1(\omega; \tau)e^{-i\omega\tau_1}, a_2(\omega; \tau)e^{-i\omega(\tau+\tau_1)}$.

The characteristic equation at E_{++} is

$$P_0(\lambda, \tau) + P_1(\lambda, \tau)e^{-\lambda\tau_1} + P_2(\lambda, \tau)e^{-\lambda(\tau+\tau_1)} = 0 \tag{5.5}$$

where $(\tau, \tau_1) \in I \times \mathbb{R}_+, I = (\tau^*, \infty)$, and

$$\begin{aligned} P_0(\lambda, \tau) &= \lambda^2 + [d + bS^*(\tau)]\lambda + bdS^*(\tau), \\ P_1(\lambda, \tau) &= -\beta S^*(\tau)[\lambda - b(1 - 2S^*(\tau))], \\ P_2(\lambda, \tau) &= \beta e^{-d\tau} S^*(\tau)[\lambda - b(1 - 2S^*(\tau))] = -e^{-d\tau} P_1(\lambda, \tau). \end{aligned}$$

In the following, we will identify the admissible values of $(\tau, \tau_1) \in (\tau^*, \infty) \times \mathbb{R}_+$ such that $\lambda = i\omega, \omega > 0$ is a zero of (5.5). Let

$$a_1(\omega, \tau) = \frac{P_1(i\omega, \tau)}{P_0(i\omega, \tau)}, \quad a_2(\omega, \tau) = -e^{-d\tau} a_1(\omega, \tau), \tag{5.6}$$

where

$$\begin{aligned} P_0(i\omega, \tau) &= bdS^*(\tau) - \omega^2 + i\omega[d + bS^*(\tau)] \neq 0, \quad \forall \omega > 0, \tau \in I, \\ P_1(i\omega, \tau) &= -\beta S^*(\tau)[i\omega - b(1 - 2S^*(\tau))]. \end{aligned} \tag{5.7}$$

Then $(i\omega, \tau, \tau_1)$ is the zero of (5.5) if and only if

$$D(\omega, \tau, \tau_1) \equiv 1 + a_1(\omega, \tau)e^{-i\omega\tau_1} + a_2(\omega, \tau)e^{-i\omega(\tau+\tau_1)} = 0. \tag{5.8}$$

Suppose that $(i\omega, \tau, \tau_1)$ is a zero of (5.5), then the three parts on the left side of (5.8) must connect to each other and form a triangle on the complex plane, as shown in Fig. 8. Therefore, we can obtain the feasible region for (ω, τ) in the following lemma.

Lemma 5.1. For $\beta > d$ and $\tau > \tau^*$, the feasible region Ω for (ω, τ) , such that $1, |a_1(\omega, \tau)|$ and $|a_2(\omega, \tau)|$ create a triangle, is

$$\Omega = \{(\omega, \tau) \in \mathbb{R}_+ \times (\tau^*, \infty) : \omega^4 + F_1(\tau)\omega^2 + F_2(\tau) \geq 0, \omega^4 + F_3(\tau)\omega^2 + F_4(\tau) \leq 0\}$$

where

$$\begin{aligned} F_1(\tau) &= b^2 S^*(\tau)^2, \\ F_2(\tau) &= b^2 d^2 (3S^*(\tau) - 1)(1 - S^*(\tau)), \\ F_3(\tau) &= d^2 + b^2 S^*(\tau)^2 - (1 + e^{-d\tau})^2 \beta^2 S^*(\tau)^2, \\ F_4(\tau) &= b^2 S^*(\tau)^2 [d^2 - (1 + e^{-d\tau})^2 \beta^2 (1 - 2S^*(\tau))^2]. \end{aligned}$$

Proof. The feasible region for (ω, τ) is also determined by (3.4). Since $|P_1(i\omega, \tau)| = e^{-b\tau} |P_2(i\omega, \tau)|$, we can see that $|P_0(\omega, \tau)| + |P_1(\omega, \tau)| \geq |P_2(\omega, \tau)|$ is always true. Moreover, it is clear that $|P_0(\omega, \tau)| + |P_2(\omega, \tau)| \geq |P_1(\omega, \tau)|$ is equivalent to

$$\omega^4 + F_1(\tau)\omega^2 + F_2(\tau) \geq 0.$$

$|P_1(\omega, \tau)| + |P_2(\omega, \tau)| \geq |P_0(\omega, \tau)|$ is equivalent to

$$\omega^4 + F_3(\tau)\omega^2 + F_4(\tau) \leq 0.$$

Therefore, the feasible region Ω is enclosed by the vertical line $\tau = \tau^*$, τ -axis, the graphs of the curves $\omega^4 + F_1(\tau)\omega^2 + F_2(\tau) = 0$ and $\omega^4 + F_3(\tau)\omega^2 + F_4(\tau) = 0$ (see the blue curves in Fig. 9(a)). □

Similarly, we consider two possible cases: 1) If $Im(a_1(\omega, \tau)e^{-i\omega\tau_1}) > 0$, then, from Fig. 8, we obtain:

$$\arg(a_1(\omega, \tau)e^{-i\omega\tau_1}) = \pi - \theta_1(\omega, \tau), \quad \arg(a_2(\omega, \tau)e^{-i\omega(\tau+\tau_1)}) = \theta_2(\omega, \tau) - \pi,$$

where $\theta_1(\omega, \tau) = \arccos G_1(\omega, \tau)$ and $\theta_2(\omega, \tau) = \arccos G_2(\omega, \tau)$, with

$$\begin{aligned} G_1(\omega, \tau) &= \frac{(\omega^2 + d^2)[\omega^2 + b^2 S^*(\tau)^2] + (1 - e^{-2d\tau})\beta^2 S^*(\tau)^2[\omega^2 + b^2(1 - 2S^*(\tau)^2)]}{2\beta S^*(\tau)\sqrt{(\omega^2 + d^2)[\omega^2 + b^2 S^*(\tau)^2][\omega^2 + b^2(1 - 2S^*(\tau)^2)}} > 0, \\ G_2(\omega, \tau) &= \frac{(\omega^2 + d^2)[\omega^2 + b^2 S^*(\tau)^2] + (e^{-2d\tau} - 1)\beta^2 S^*(\tau)^2[\omega^2 + b^2(1 - 2S^*(\tau)^2)]}{2e^{-d\tau}\beta S^*(\tau)\sqrt{(\omega^2 + d^2)[\omega^2 + b^2 S^*(\tau)^2][\omega^2 + b^2(1 - 2S^*(\tau)^2)}}. \end{aligned}$$

Hence, we get there is an $n \in \mathbb{Z}$, such that

$$\arg(a_2(\omega, \tau)) - \arg(a_1(\omega, \tau)) - [\theta_1(\omega, \tau) + \theta_2(\omega, \tau)] + 2n\pi = \omega\tau \tag{5.9}$$

and

$$\tau_1 = \frac{1}{\omega} [\arg(a_1(\omega, \tau)) + \theta_1(\omega, \tau) + (2j - 1)\pi], \quad j \geq j_0^+, \tag{5.10}$$

where j_0^+ is the smallest integer such that $\tau_1 > 0$ and τ is the zero of (5.9).

2) If $Im(a_1(\omega, \tau)e^{-i\omega\tau}) < 0$, the triangular formed by 1, $a_1(\omega, \tau)e^{-i\omega\tau}$ and $a_2(\omega, \tau)e^{-i\omega(\tau+\tau_1)}$ is the mirror image of the one in Fig. 1 about the real axis. Therefore, we obtain

$$\arg(a_2(\omega, \tau)) - \arg(a_1(\omega, \tau)) + [\theta_1(\omega, \tau) + \theta_2(\omega, \tau)] + 2n\pi = \omega\tau, \quad (5.11)$$

and

$$\tau_1 = \frac{1}{\omega} [\arg(a_1(\omega, \tau)) - \theta_1(\omega, \tau) + (2j - 1)\pi], \quad j \geq j_0^-, \quad (5.12)$$

where j_0^- is the smallest integer such that $\tau_1 > 0$.

We denote by I_ω the interval of ω for the feasible region Ω and I_ω^τ the feasible values of τ for each fixed $\omega \in I_\omega$. Now, for fixed $\omega \in I_\omega$ and $n \in \mathbb{Z}$, we can introduce the functions of τ , say $S_n^\pm : I_\omega^\tau \rightarrow \mathbb{R}$, as

$$S_n^\pm(\omega, \tau) = \tau - \frac{1}{\omega} [\arg(a_2(\omega, \tau)) - \arg(a_1(\omega, \tau)) \mp (\theta_1(\omega, \tau) + \theta_2(\omega, \tau)) + 2n\pi]. \quad (5.13)$$

We write the zeros of (5.13), if it exists, as $\hat{\tau}^{i\pm}(\omega)$, $i = 1, 2, \dots$. Then we can set up the corresponding τ_1 values as follows:

$$\hat{\tau}_{1,i}^{j\pm}(\omega) = [\arg(a_1(\omega, \hat{\tau}^{i\pm})) \pm \theta_2(\omega, \hat{\tau}^{i\pm}) + (2j^\pm - 1)\pi] / \omega, \quad (5.14)$$

for $j = j_0^\pm, j_0^\pm + 1, \dots$, where j_0^\pm is the smallest integer such that $\hat{\tau}_{1,i}^{j\pm}(\omega) > 0$.

When ω takes the values throughout the interval I_ω , then we get the curve

$$\mathcal{C} := \{(\omega, \hat{\tau}^{i\pm}(\omega)) : \omega \in I_\omega, S_n^\pm(\omega, \hat{\tau}^{i\pm}(\omega)) = 0\} \quad (5.15)$$

on Ω (see Fig. 9(a)), which will later determine the shape of the crossing curves

$$\mathcal{T} = \{(\hat{\tau}^{i\pm}(\omega), \hat{\tau}_{1,i}^{j\pm}(\omega)) \in (\tau^*, \infty) \times \mathbb{R}_+ | \omega \in I_\omega\}, \quad (5.16)$$

on (τ, τ_1) -plane (see Fig. 9(b)).

Remark 5.2. Recall that we assume m_1 is sufficiently small. Therefore, the crossing curves for the original model (5.3) should be perturbations of the crossing curves defined in (5.16), when τ_1 is not large enough.

Remark 5.3. For the transcendental equation (5.1), by an analysis similar to Section 3, one can see that looped connected segment in Ω must be formed by two components of \mathcal{C} in the same type AA, BB, CC or BC. Moreover, taking slight modifications to the proofs of Propositions 3.12 and 3.13, we can derive that the Propositions 3.12, 3.13 and Theorem 3.14 remains true for (5.1).

Finally, in order to study the variation of the pure imaginary eigenvalues of (5.1) (or (5.5), (5.8)) with the time delay (τ, τ_1) , we should calculate the crossing direction of the crossing curve (5.16). Based on the analysis in Section 4, we need to judge the sign of

$$R(\tau, \tau_1)I_1(\tau, \tau_1) - R_1(\tau, \tau_1)I(\tau, \tau_1),$$

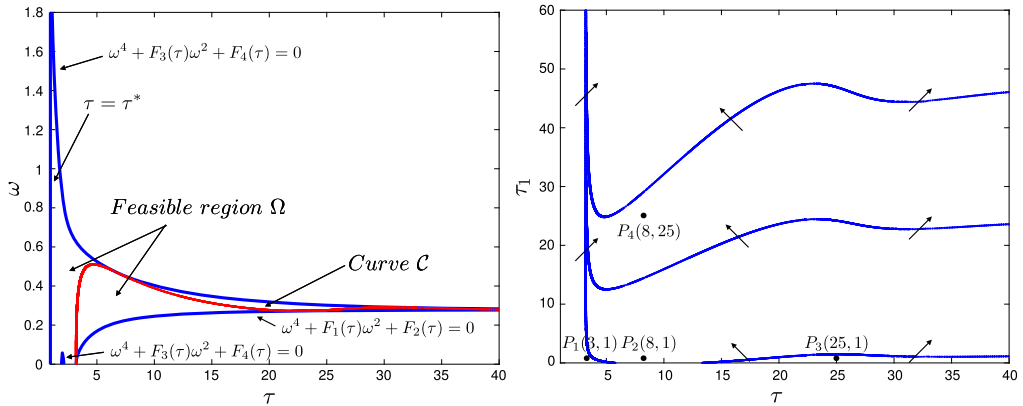


Fig. 9. (a) Feasible region Ω and the Curve \mathcal{C} , which is composed by the admissible values of (ω, τ) . (b) Crossing curve and crossing direction.

where R, R_1, I, I_1 are defined by (4.1) with D in the form of (5.1). Benefit from

$$R(\tau, \tau_1)I_1(\tau, \tau_1) - R_1(\tau, \tau_1)I(\tau, \tau_1) = -\text{Im} \left\{ \frac{\partial D}{\partial \tau} \cdot \overline{\frac{\partial D}{\partial \tau_1}} \right\},$$

we obtain the following results.

Theorem 5.4. *The characteristic equation (5.5) admits a pair of conjugate roots $\pm i\omega^*$, for $(\tau, \tau_1) = (\tau^*, \tau_1^*) \in \mathcal{T}$. Denote by $\lambda^\pm(\tau, \tau_1) = \alpha(\tau, \tau_1) \pm i\omega(\tau, \tau_1)$ the pair of conjugate complex roots of (5.5) in some neighborhood of (τ^*, τ_1^*) , such that $\alpha(\tau^*, \tau_1^*) = 0$ and $\omega(\tau^*, \tau_1^*) = \omega^*$. If $\delta(\tau^*, \tau_1^*) > 0$ ($\delta(\tau^*, \tau_1^*) < 0$), then $\lambda^\pm(\tau, \tau_1)$ cross the imaginary axis from left to right, as (τ, τ_1) passes through the crossing curve to the region on the right (left), where*

$$\delta(\tau^*, \tau_1^*) = -\text{Re} \left\{ \left[P_{0\tau}^* + P_{1\tau}^* e^{-i\omega^* \tau_1^*} + (P_{2\tau}^* - i\omega^* P_2^*) e^{-i\omega^*(\tau^* + \tau_1^*)} \right] \left[\overline{P_1^* e^{i\omega^* \tau_1^*} + P_2^* e^{i\omega^*(\tau^* + \tau_1^*)}} \right] \right\},$$

with $P_l^* = P_l(i\omega^*, \tau^*)$ and $P_{l\tau}^* = \frac{\partial P_l}{\partial \tau}(i\omega^*, \tau^*)$, $l = 0, 1, 2$.

Example 5.5. Let $b = 1, d = 0.1$ and $\beta = 1$ in the epidemic model (5.4). According to Lemma 5.1, we obtain the feasible region Ω for (ω, τ) , which is enclosed by the blue curves and τ -axis in Fig. 9(a). Then, searching the zeros of (5.13) for each $\omega \in I_\omega$, the curve \mathcal{C} , which is composed by the admissible values of (ω, τ) , can be achieved, see the red curve in Fig. 9(a). Through an analysis similar to Proposition 3.12, we can see the open-ended curve \mathcal{C} on Ω leads to a series of open ended crossing curves \mathcal{T} on (τ, τ_1) -plane, and it has been shown in Fig. 9(b). Finally, we calculate the crossing direction in the light of Theorem 5.4 and present the final result in Fig. 9(b), that is, when (τ, τ_1) changes along the direction of the arrows, then the characteristic roots $\lambda^\pm(\tau, \tau_1)$ passes through the imaginary axis from left to right.

In Fig. 10, we choose points $P_1 - P_4$ in Fig. 9(b) as the values of (τ, τ_1) , to simulate the dynamical behaviors of model (5.4). We observed the stability switch when (τ, τ_1) takes the values from P_1 and P_2 to P_3 . Moreover, the quasi-period oscillation has been found when the values of (τ, τ_1) are chosen above the second crossing curve in Fig. 9(b).

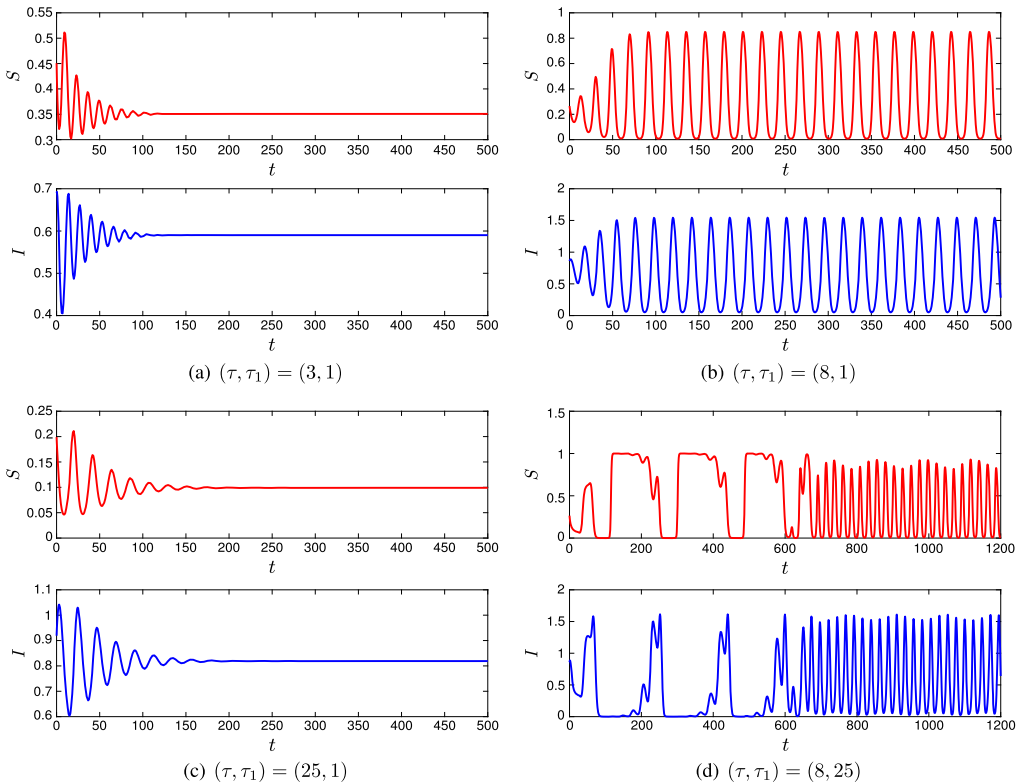


Fig. 10. The dynamics of model (5.4) with different values of (τ, τ_1) . Here $b = 1, d = 0.1, \beta = 1$ and initial functions are $(S^*(\tau) + 0.1, I^*(\tau) + 0.1)$ for $t \in [-\max\{\tau, \tau_1\}, 0)$. When $\tau_1 = 1$ is fixed, the stability of E_{++} changes from stable to unstable, and then to stable again as the value of τ increases. Furthermore, the quasi-periodic solution can be obtained when the values of (τ, τ_1) are chosen above the middle crossing curve in Fig. 9(b).

6. Discussion

In this paper, we extend the geometric method established in [5] to a more general transcendental equation (2.1), involving two time delays and delay-dependent parameters. This allows us to find crossing curves in (τ, τ_1) -plane on which (2.1) has purely imaginary roots, whereas determining such curves is more complicated than that of [5]. We prove that the crossing curves essentially include four types: open-ended, closed, spiral-like curves and truncated curves. The steps for determining the crossing curves are summarized as follows:

1. Determining the feasible region Ω for (ω, τ) , based on (3.3) or (3.4). The admissible range of ω for each connected region of Ω are denoted by $I_k, k = 1, 2, \dots, N$.
2. For each fixed $\omega \in I_k$, identify the zeros of the S_n^\pm in I_ω^k , and let ω take all the feasible values. Then, we get the curve $\mathcal{C} := \{(\omega, \hat{\tau}^{i^\pm}(\omega)) : \omega \in I_k, S_n^\pm(\omega, \hat{\tau}^{i^\pm}(\omega)) = 0\}$ on Ω , which will not only determine the shape of the crossing curve, but also show the positive direction of the crossing curve.
3. For each $\hat{\tau}^{i^\pm}(\omega)$, set up the corresponding values of τ_1 by (3.14), to obtain the crossing curve $\mathcal{T} = \{(\hat{\tau}^{i^\pm}(\omega), \hat{\tau}_{1,i}^{j^\pm}(\omega)) \in I_\omega \times \mathbb{R}_+ | \omega \in I_k\}$.
4. Calculate the crossing directions of the crossing curve according to Theorem 4.1.

The critical step in the above process is to determine the curve \mathcal{C} on Ω . Each point on \mathcal{C} is a zero of the function $S_n^\pm(\omega, \tau)$, which is in general to be solved with the aid of numerical simulation due to the complexity of the expression for $S_n^\pm(\omega, \tau)$. Once \mathcal{C} is obtained, the shape of the crossing curves will be immediately concluded by Propositions 3.12 and 3.13.

Note that the results of this paper include the results presented by Gu et al. [5] for the characteristic equation with two time-delay and parameters independent of delay:

$$D(\lambda, \tau, \tau_1) := P_0(\lambda) + P_1(\lambda)e^{-\lambda\tau} + P_2(\lambda)e^{-\lambda\tau_1} = 0. \tag{6.1}$$

For (6.1), the feasible region for (ω, τ) must be one or several strips, which are unbounded in the direction of τ -axis. Moreover, since a_1 and θ_1 in (3.12) become independent of τ as assumed in [5], we can see (3.12) has infinitely many zeros for each fixed $\omega \in I_k$. Therefore, the curve \mathcal{C} can be composed by one unbounded open-ended segment (similar to right side of Fig. 6(a)) or a series of unbounded open-ended segments (similar to right side of Fig. A.13) or a series of looped segments (similar to right side of Fig. A.15). Furthermore, it is easy to see that each component of the open-ended curve segment must be Type AC or BC. Then, according to the proofs of Propositions 3.12–3.13, one can deduce the classifications of crossing curves as the Proposition 4.5 in [5]. Furthermore, the function $\delta(\tau, \tau_1)$ used to judge the crossing direction in Theorem 4.1 is now reduced to

$$\delta(\tau, \tau_1) = -\text{Im}\{P_1 \overline{P_2} e^{\lambda(\tau_1 - \tau)}\},$$

from which the Proposition 6.1 in [5] can be derived.

This geometric method is also applicable to the transcendental equations with the form of

$$D(\lambda, \tau, \tau_1) := P_0(\lambda, \tau) + P_1(\lambda, \tau)e^{-\lambda\tau} + P_2(\lambda, \tau)e^{-\lambda(\tau + \tau_1)} = 0. \tag{6.2}$$

Similarly, by taking the same transformation as (3.2), we can observe that the feasible region for (ω, τ) of (6.2) is also determined by (3.3) or (3.4). Suppose that $(i\omega, \tau, \tau_1)$ is a zero of (6.2), then we have

$$\arg(a_1(\omega, \tau)e^{-i\omega\tau}) = \pi - \theta_1(\omega, \tau), \quad \arg(a_2(\omega, \tau)e^{-i\omega(\tau + \tau_1)}) = \theta_2(\omega, \tau) - \pi,$$

or

$$\arg(a_1(\omega, \tau)e^{-i\omega\tau}) = \theta_1(\omega, \tau) - \pi, \quad \arg(a_2(\omega, \tau)e^{-i\omega(\tau + \tau_1)}) = \pi - \theta_2(\omega, \tau).$$

Therefore, we can define the functions of S_n^\pm as (3.12). For fixed $\omega \in I_k$, we also denote the zeros of S_n^\pm by $\hat{\tau}^{i\pm}(\omega)$. However, now the admissible values of τ_1 should be defined as follows:

$$\hat{\tau}_{1,i}^{j\pm}(\omega) = [\arg(a_2(\omega, \hat{\tau}^{i\pm})) - \omega\hat{\tau}^{i\pm} + (2j^\pm - 1)\pi \mp \theta_2(\omega, \hat{\tau}^{i\pm})]/\omega. \tag{6.3}$$

Making some minor changes to the discussion in Section 3, we propose the conjecture that Theorem 3.14 is also valid for (6.2). For the crossing direction, we assert that the function $\delta(\tau, \tau_1)$ in Theorem 4.1 for (6.2) is now

$$\delta(\tau, \tau_1) = -\text{Re} \left\{ \left[\frac{\partial P_0}{\partial \tau} e^{\lambda(\tau + \tau_1)} + \left(\frac{\partial P_1}{\partial \tau} - \lambda P_1 \right) e^{\lambda\tau_1} + \left(\frac{\partial P_2}{\partial \tau} - \lambda P_2 \right) \right] \overline{P_2} \right\}.$$

In addition, for a system with single time delay and k equations, if the equilibrium is delay dependent, then the corresponding characteristic equation can take the following form:

$$D(\lambda, \tau, \tau_1) := P_0(\lambda, \tau) + P_1(\lambda, \tau)e^{-\lambda\tau} + P_2(\lambda, \tau)e^{-\lambda k\tau} = 0. \tag{6.4}$$

When $k = 1$, (6.4) reduces to $D(\lambda, \tau, \tau_1) := P_0(\lambda, \tau) + Q(\lambda, \tau)e^{-\lambda\tau} = 0$ with $Q(\lambda, \tau) = P_1(\lambda, \tau) + P_2(\lambda, \tau)$, which has been studied by Beretta and Kuang [8]. Subsequently, Beretta and Tang [29] extended the method developed in [8] to the case of $k = 2$. For $k \geq 3$, there exist no mathematical results or methods as we are aware of. However, for $\tau_1 = k\tau$, the geometric method presented in this paper can easily be applied to all integers $k \geq 1$.

In the end, we would like to mention that the characteristic equation for a two-delay model with delay dependent parameters can have a more complicated characteristic equation than (2.1), for instance,

$$P_0(\lambda, \tau) + P_1(\lambda, \tau)e^{-\lambda\tau} + P_2(\lambda, \tau)e^{-\lambda\tau_1} + P_3(\lambda, \tau)e^{-\lambda(\tau+\tau_1)} = 0. \tag{6.5}$$

The idea of the proposed geometric method can also apply to (6.5). However, far more complicated analysis needs to be preformed in this case since we will encounter a quadrilateral constructed by the four terms on the left hand side of (6.5).

Appendix A. Various types of crossing curves

In this appendix, we present different types of crossing curves by the following examples.

Example A.1. Choose

$$P_0(\lambda, \tau) = \lambda + 0.6, \quad P_1(\lambda, \tau) = 8e^{-0.5\tau}, \quad P_3(\lambda, \tau) = 2e^{-0.1\tau}.$$

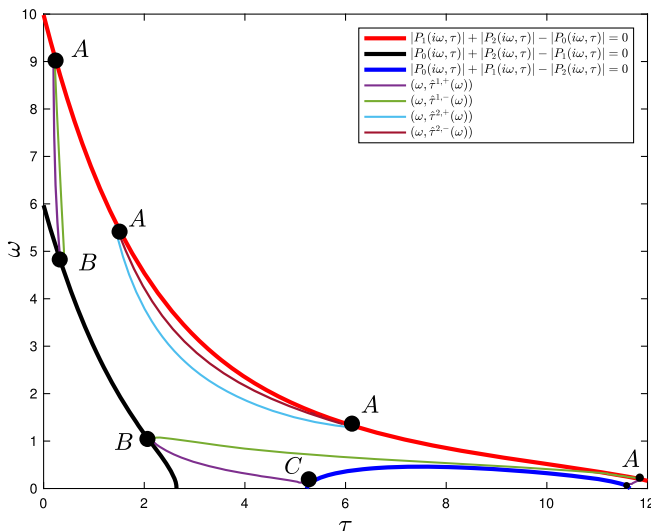


Fig. A.11. Feasible region and the curve C for Example A.1.

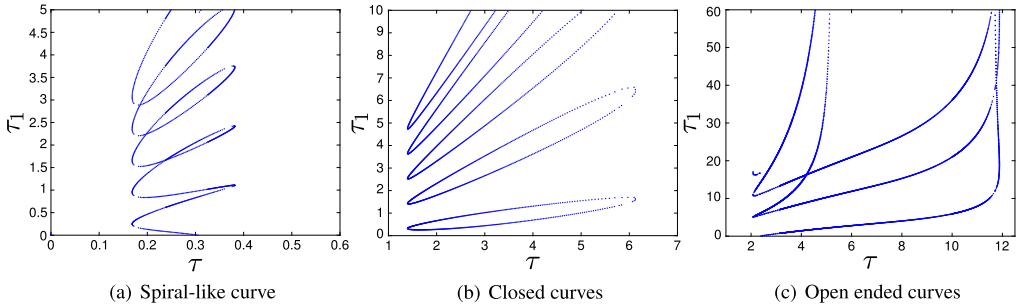


Fig. A.12. Different types of crossing curves for Example A.1.

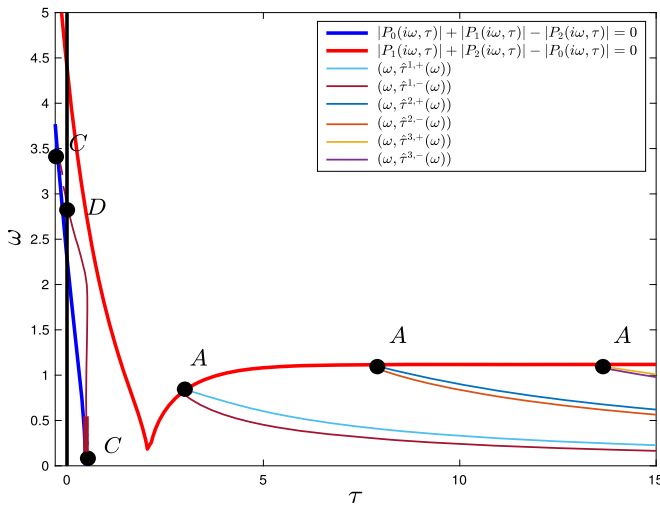


Fig. A.13. Feasible region and the curve C for Example A.2.

As shown in Fig. A.11, the curve C involves two closed loops (one loop is formed by two curves of Type AB, and another is formed by two curves of Type AA), and one open ended curve connected by three components of Type AB, BC and AC. Therefore, the crossing curves could include the first three cases in Theorem 3.14: a spiral-like curve (associated with the left loop of C in Fig. A.11); a series of closed curves (associated with the right loop); and a series of open ended curves. These three types of crossing curves are illustrated separately in Fig. A.12, for the purpose of better visualization. One can also compute the crossing directions as in previous example, which are omitted here.

Example A.2. For (2.1), let

$$P_0(\lambda, \tau) = \lambda + 1, \quad P_1(\lambda, \tau) = 1, \quad P_2(\lambda, \tau) = 4e^{-\tau} - 0.5.$$

It is observed in Fig. A.13, the curve C consisting of a truncated component and a series of opened curves with two components. The truncated curve touches ω -axis at one end. If this end is extended leftward until it reaches one of the blue curve again, then we observe that it is of

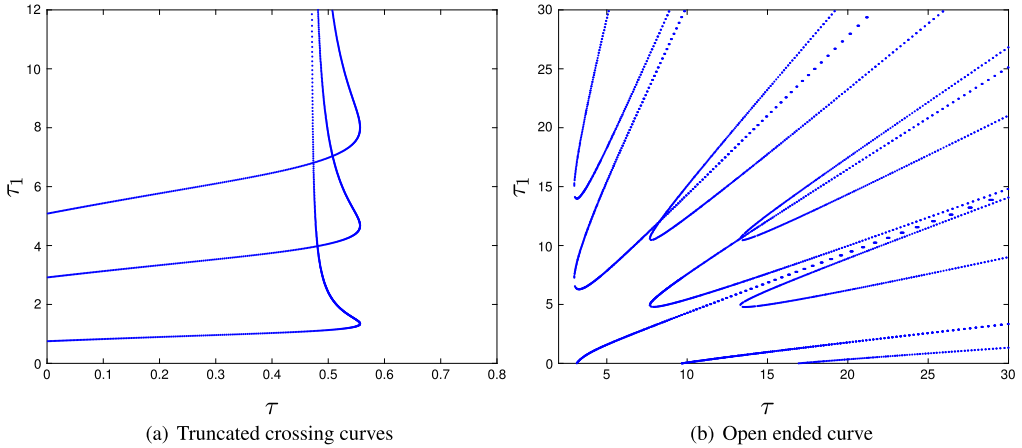


Fig. A.14. Different types of crossing curves for Example A.2.

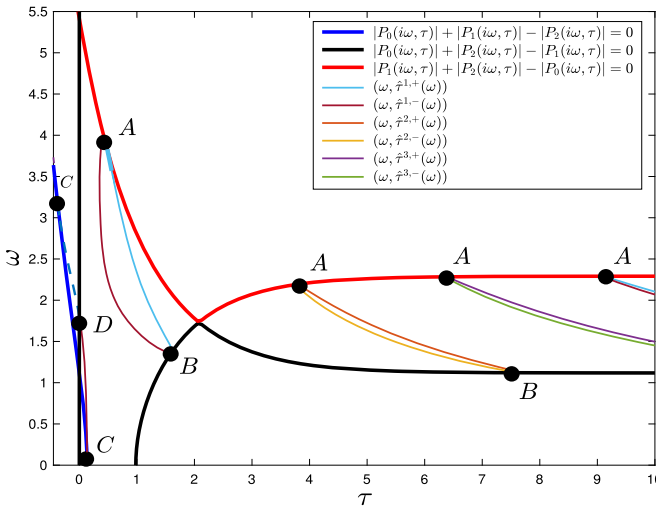


Fig. A.15. Feasible region and the curve C for Example A.3.

Type CC. Therefore, the extended crossing curves are a series of open ended curves, so are the truncated ones, see Fig. A.14(a). According to Proposition 3.12, the unbounded opened curves with finitely many components form a series of open ended crossing curves that can spread out in the direction of τ -axis, see Fig. A.14(b).

Example A.3. Consider the system (2.1) with

$$P_0(\lambda, \tau) = \lambda + 1, \quad P_1(\lambda, \tau) = 2, \quad P_2(\lambda, \tau) = 4e^{-\tau} - 0.5.$$

The curve C is shown in Fig. A.15. According to Proposition 3.12–3.13, the crossing curves contains a series of truncated curves (see Fig. A.16(a)) and a series of spiral-like curve along the τ_1 -axis (see Fig. A.16(b)–A.16(c)).

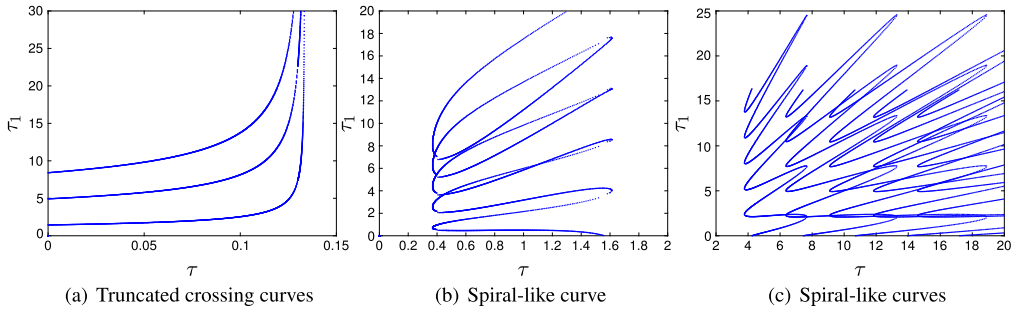


Fig. A.16. Different types of crossing curves for Example A.3.

References

- [1] R.E. Bellman, K.L. Cooke, *Differential-Difference Equations*, Academic Press, New York–London, 1963.
- [2] Y. Kuang, *Delay Differential Equations with Applications in Population Dynamics*, Mathematics in Science and Engineering, Academic Press, Inc., Boston, MA, 1993.
- [3] Y. Kuang, J.D. Nagy, S.E. Eikenberry, *Introduction to Mathematical Oncology*, Chapman & Hall/CRC Mathematical and Computational Biology Series, CRC Press, Boca Raton, FL, 2016.
- [4] H. Smith, *An Introduction to Delay Differential Equations with Applications to the Life Sciences*, Texts in Applied Mathematics, Springer, New York, 2011.
- [5] K. Gu, S. Niculescu, J. Chen, On stability crossing curves for general systems with two delays, *J. Math. Anal. Appl.* 311 (1) (2005) 231–253.
- [6] J. Li, Y. Kuang, C. Mason, Modeling the glucose and insulin regulatory system and ultradian insulin secretory oscillations with two time delays, *J. Theoret. Biol.* 242 (3) (2006) 722–735.
- [7] J. Bélair, M.C. Mackey, J.M. Mahaffy, Age-structured and two-delay models for erythropoiesis, *Math. Biosci.* 128 (1–2) (1995) 317.
- [8] S.A. Gourley, Y. Kuang, A stage structured predator-prey model and its dependence on maturation delay and death rate, *J. Math. Biol.* 49 (2) (2004) 188–200.
- [9] Y. Kuang, J.W.-H. So, Analysis of a delayed two-stage population model with space-limited recruitment, *SIAM J. Appl. Math.* 55 (6) (1995) 1675–1696.
- [10] S.L. Robertson, S.M. Henson, T. Robertson, J.M. Cushing, A matter of maturity: to delay or not to delay? Continuous-time compartmental models of structured populations in the literature 2000–2016, *Nat. Resour. Model.* 31 (1) (2018) e12160, 26.
- [11] R.A. Everett, J.D. Nagy, Y. Kuang, Dynamics of a data based ovarian cancer growth and treatment model with time delay, *J. Dynam. Differential Equations* 28 (3–4) (2016) 1393–1414.
- [12] X. Shi, Y. Kuang, A. Makroglou, S. Mokshagundam, J. Li, Oscillatory dynamics of an intravenous glucose tolerance test model with delay interval, *Chaos* 27 (11) (2017) 114324.
- [13] S.A. Gourley, Y. Kuang, Wavefronts and global stability in a time-delayed population model with stage structure, *Proc. R. Soc. Lond. Ser. A Math. Phys. Eng. Sci.* 459 (2034) (2003) 1563–1579.
- [14] K.L. Cooke, Z. Grossman, Discrete delay, distributed delay and stability switches, *J. Math. Anal. Appl.* 86 (2) (1982) 592–627.
- [15] H.I. Freedman, Y. Kuang, Stability switches in linear scalar neutral delay equations, *Funkcial. Ekvac.* 34 (2) (1991) 187–209.
- [16] J. Li, Y. Kuang, Analysis of a model of the glucose-insulin regulatory system with two delays, *SIAM J. Appl. Math.* 67 (3) (2007) 757–776.
- [17] X. Lin, H. Wang, Stability analysis of delay differential equations with two discrete delays, *Can. Appl. Math. Q.* 20 (4) (2012) 519–533.
- [18] S. Chen, J. Shi, J. Wei, Time delay-induced instabilities and Hopf bifurcations in general reaction–diffusion systems, *J. Nonlinear Sci.* 23 (1) (2013) 1–38.
- [19] E. Beretta, Y. Kuang, Geometric stability switch criteria in delay differential systems with delay dependent parameters, *SIAM J. Math. Anal.* 33 (5) (2002) 1144–1165.
- [20] C. Jin, K. Gu, I. Boussaada, S. Niculescu, Stability analysis of a more general class of systems with delay-dependent coefficients, *IEEE Trans. Automat. Control* (2018).

- [21] H. Miao, Z. Teng, C. Kang, Stability and Hopf bifurcation of an HIV infection model with saturation incidence and two delays, *Discrete Contin. Dyn. Syst. Ser. B* 22 (6) (2017) 2365–2387.
- [22] X. Xu, J. Wei, Bifurcation analysis of a spruce budworm model with diffusion and physiological structures, *J. Differential Equations* 262 (10) (2017) 5206–5230.
- [23] C. Jin, K. Gu, S. Niculescu, I. Boussaada, Stability analysis of systems with delay-dependent coefficients: an overview, *IEEE Access* 6 (2018) 27392–27407, <https://doi.org/10.1109/ACCESS.2018.2828871>.
- [24] J.K. Hale, W. Huang, Global geometry of the stable regions for two delay differential equations, *J. Math. Anal. Appl.* 178 (2) (1993) 344–362.
- [25] J. Bélair, S.A. Campbell, Stability and bifurcations of equilibria in a multiple-delayed differential equation, *SIAM J. Appl. Math.* 54 (5) (1994) 1402–1424.
- [26] J.M. Mahaffy, K.M. Joiner, P.J. Zak, A geometric analysis of stability regions for a linear differential equation with two delays, *Internat. J. Bifur. Chaos Appl. Sci. Engrg.* 5 (3) (1995) 779–796.
- [27] X. Li, S. Ruan, J. Wei, Stability and bifurcation in delay-differential equations with two delays, *J. Math. Anal. Appl.* 236 (2) (1999) 254–280.
- [28] S. Ruan, J. Wei, On the zeros of transcendental functions with applications to stability of delay differential equations with two delays, *Dyn. Contin. Discrete Impuls. Syst. Ser. A Math. Anal.* 10 (6) (2003) 863–874.
- [29] E. Beretta, Y. Tang, Extension of a geometric stability switch criterion, *Funkcial. Ekvac.* 46 (3) (2003) 337–361.